Macrophage-Epithelial Interactions during Influenza Virus Pneumonia: Alveolar Recruitment Pathways and Impact on Epithelial Barrier Integrity

Inaugural Dissertation

submitted to the

Faculty of Medicine

in partial fulfillment of the requirements

for the PhD-Degree

of the Faculties of Veterinary Medicine and Medicine

of the Justus Liebig University Giessen

by

Dr. Susanne Valerie Herold

from

Offenburg

Giessen, July 17th, 2008

From the Department of Internal Medicine II

Director: Prof. Dr. W. Seeger

of the Faculty of Medicine of the Justus Liebig University Giessen

First Supervisor and Committee Member: Prof. Dr. J. Lohmeyer

Second Supervisor and Committee Member: Prof. Dr. O. Planz

Committee Members:

Prof. Dr. H.-J. Thiel

Prof. Dr. S. Pleschka

Date of Doctoral Defense: Oct. 17th, 2008

Abbreviations

AEC	alveolar epithelial cells
ALI	acute lung injury
ARDS	adult respiratory distress syndrome
BAL(F)	bronchoalveolar lavage (fluid)
CCR2/5	CC chemokine receptor 2/5
CCL2/5	CC chemokine ligand 2/5
DC	dendritic cells
(d)pi	(days) post infection
DR5	death receptor 5
Ex-Ma	exudate macrophage
FasL	Fas ligand
FP	forward primer
HPAIV	highly pathogenic avian influenza virus
HRP	horse radish peroxidase
im	intramuscular
ip	intraperitoneal
IV	influenza virus
mAb	monoclonal antibody
MACS	magnetic cell separation
mn	mononuclear
MOI	multiplicity of infection
PB-Mo	peripheral blood monocyte
PFU	plaque forming units
PR/8	A/PR/8/34
(r)AM	(resident) alveolar macrophage
RP	reverse primer
rpm	rounds per minute
RT	room temperature
TNF-α	tumor necrosis factor-alpha
TRAIL	TNF-related apoptosis-inducing ligand
SSC	side scatter
wt	wildtype

1. Introduction

1.1 Influenza A virus

Influenza A virus (IV) is a highly contagious RNA virus causing infection of the human respiratory tract. IV infections have been recognized as a major cause of morbidity and mortality, especially in the very young, the very old and in immunocompromised individuals. Each year, influenza infections result in 3 - 5 million cases of severe illness and kill 250,000 - 500,000 people worldwide, hence representing a major social and economic burden (1). Apart from annual epidemics, three major pandemics spread around the globe in the 20th century, affecting primarily young and previously healthy adults. The Spanish Flu in 1918/19 resulted in the deaths of 50 - 100 million people (2). Further pandemics occurred in 1957 (Asian Flu) and 1968 (Hong Kong Flu).

Influenza A viruses contain eight independent single-stranded RNA segments of negative polarity packaged in the viral core and coding for 11 proteins: hemagglutinin, neuraminidase, nucleoprotein, matrix proteins 1 and 2, non-structural proteins 1 and 2, polymerase A, polymerase B1, polymerase B1-F2, and polymerase B2 (3). The core is surrounded by a lipid envelope derived from the plasma membrane of infected host cells during the process of budding from the cellular surface (Fig. 1). Influenza A viruses belong to the family of orthomyxoviridae and are classified according to their surface glycoprotein molecules hemagglutinin (HA) and neuraminidase (NA). Sixteen different hemagglutinin and nine neuraminidase variants are known, but only subtypes A/H1N1 and A/H3N2 are usually circulating in the human population. However, in recent years, highly pathogenic influenza viruses have evolved from avian H5 or H7 strains in South-East Asia by occasional point mutations in the viral genome (antigenic drift) and genetic reassortment between different influenza viruses (antigenic shift) (4). A/H5N1 strains infected humans during outbreaks in 1997 and 2004/5, raising pandemic concern. Highly pathogenic avian influenza viruses (HPAIV), in contrast to "classical" human strains, are characterized by an early spread from the upper to the lower respiratory tract. By virtue of their high replication efficiency and their ability to attach to and infect distal respiratory epithelial cells, HPAIV cause primary viral pneumonia with rapid progression to lung failure and fatal outcome (5-9). Besides direct

viral cytopathic effects, the contribution of host immune response factors to acute lung injury during IV pneumonia has been discussed (10, 11).
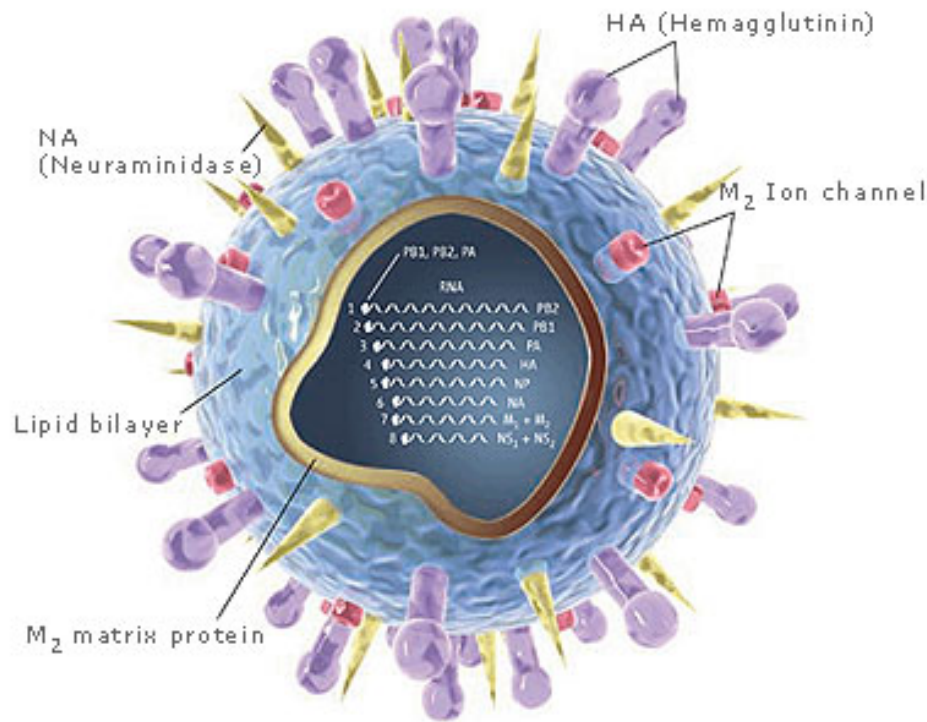
Fig. 1. Structural diagram of influenza virus (modified from Kaiser, J., Science Vol. 312, page 380).

1.2 Host immune response to influenza A virus infection

Influenza A virus pneumonia is characterized by an early influx of neutrophils followed by the recruitment of large numbers of blood-derived monocytes within the first days of infection. During later stages, CD8+ cytotoxic T lymphocytes from mediastinal lymph nodes accumulate within inflamed lungs. The accumulation of large numbers of monocytes within the lung parenchyma and alveolar spaces has been described as a hallmark of host defense during viral infection initiating adaptive immune responses and thereby limiting viral spread (9, 12-18). The process of inflammatory leukocyte recruitment towards the lungs in response to IV infection is initiated by the release of early proinflammatory cytokines such as IFN-α/ß (interferon-α/ß), TNF-α (tumor necrosis factor-α) and interleukin-1 (IL-1) together with a variety of chemokines like CCL2 (MCP-1, monocyte chemoattractant protein-1), CCL5 (RANTES, regulated upon

activation, normal T cell expressed and secreted), CCL3/4 (MIP-1α/β, macrophage inflammatory protein-1α/β), CXCL10 (IP-10, interferon-inducible protein-10) and CXCL8 (IL-8, interleukin 8) from infected resident alveolar macrophages and lung epithelial cells (16-24). Chemokines are small cytokines that have been shown to act as selective chemoattractants for leukocyte subpopulations *in vitro* and to elicit the accumulation of inflammatory cells *in vivo*. The chemokine superfamily can be divided into four groups (CXC, CX$_3$C, CC, and C) according to the positioning of the first two closely paired and highly conserved cysteines of the amino acid sequence (25). Particularly the CC chemokines CCL2 and CCL5 are major monocyte chemoattractants acting via the CC chemokine receptors CCR2 and CCR5, respectively (26-29). Chemokine receptors belong to the family of G protein-coupled seven-transmembrane-spanning receptors and are primarily expressed on hemopoietic cells, but as well on parenchymal lung cells (30). Upon ligand binding, a rise in intracellular calcium flux activates specific cellular pathways involved in chemotaxis and changes in the avidity of cellular adhesion molecules, thus mediating the binding to endo- and epithelial cells and the migration into inflamed tissues (31). However, the chemokine-receptor interactions involved in alveolar monocyte transmigration during IV pneumonia and the role of IV infected resident alveolar epithelial cells in this context remain unclear so far.

1.3 The lung mononuclear phagocyte system

Peripheral blood monocytes are circulating precursors of tissue macrophages and dendritic cells and, together with the latter, have collectively been termed "the mononuclear phagocyte system". Mononuclear phagocytes are long living cells with broad differentiation potential entering lung tissue by two pathways: (i) constitutively to regenerate resident alveolar macrophage (rAM) and lung dendritic cell (DC) pools and (ii) inflammation-driven to initiate and support immune responses (32). Forming the first line of defense against invading pathogens, mononuclear phagocytes have been attributed a crucial role in pulmonary host defense (33).

Two major circulating monocyte subsets that vary in chemokine receptor and adhesion molecule expression, as well as in migratory and differentiation

properties, have been identified. In humans, inflammatory $CD14^+CD16^-$ monocytes express CCR2, CD64, and CD62L, whereas non-inflammatory $CD14^{low}CD16^+$ monocytes lack CCR2. Their counterparts in mice are $CX_3CR1^-CCR2^+GR1^{high}$ and $CX_3CR1^+CCR2^-GR1^{low}$ monocytes, respectively. $GR1^{high}$ monocytes are recruited to inflammatory sites, e.g. atherosclerotic lesions, inflamed skin or acutely inflamed peritoneum giving rise to tissue macrophages and DCs in inflammatory or infectious disease models and to epidermal Langerhans cells after skin inflammation. In contrast, $GR1^{low}$ monocytes develop into tissue macrophages under non-inflammatory conditions (34-39).

The mononuclear phagocyte system of the murine lung is composed of resident interstitial and alveolar macrophages ($F4/80^+GR1^{low}CD11c^{high}MHCII^{low}$) and pulmonary dendritic cells ($F4/80^+GR1^{high}CD11c^{high}MHCII^{high}$), both derived from a common $CD117^+$ bone marrow precursor (40, 41). Under steady state conditions, resident lung macrophages derive from the $CX_3CR1^+CCR2^-GR1^{low}$ peripheral blood monocyte subset with a slow turnover rate of approximately 40% per year (42). During lung inflammation and infection, $CX_3CR1^-CCR2^+GR1^{high}$ blood monocytes ($F4/80^+CD11c^-CD11b^+CD115^+$) are rapidly recruited to the alveolar compartment of the lung (14, 36, 43). These "exudate" macrophages ($F4/80^+GR1^{high}CD11c^{int}MHCII^{low}$) acquire a lung resident macrophage phenotype and finally replenish the alveolar macrophage pool during the time course of infection (42, 44)(Fig.2).

Besides their essential host defense functions, mononuclear phagocytes have been proposed to contribute to an imbalanced, detrimental immune response during IV pneumonia (10, 45), presumably resulting in alveolar epithelial damage. Human influenza virus pneumonia is characterized by acute mononuclear alveolitis followed by massive pulmonary oedema, hemorrhage and extensive destruction of the respiratory epithelium with impaired blood oxygenation and multi-organ failure (9, 46, 47). However, the distinct molecular steps during macrophage-epithelial cross-talk that lead to severe damage of the highly sensitive gas exchange compartment during IV-induced acute lung injury (ALI) or its more severe form, ARDS (adult respiratory distress syndrome), remain elusive.
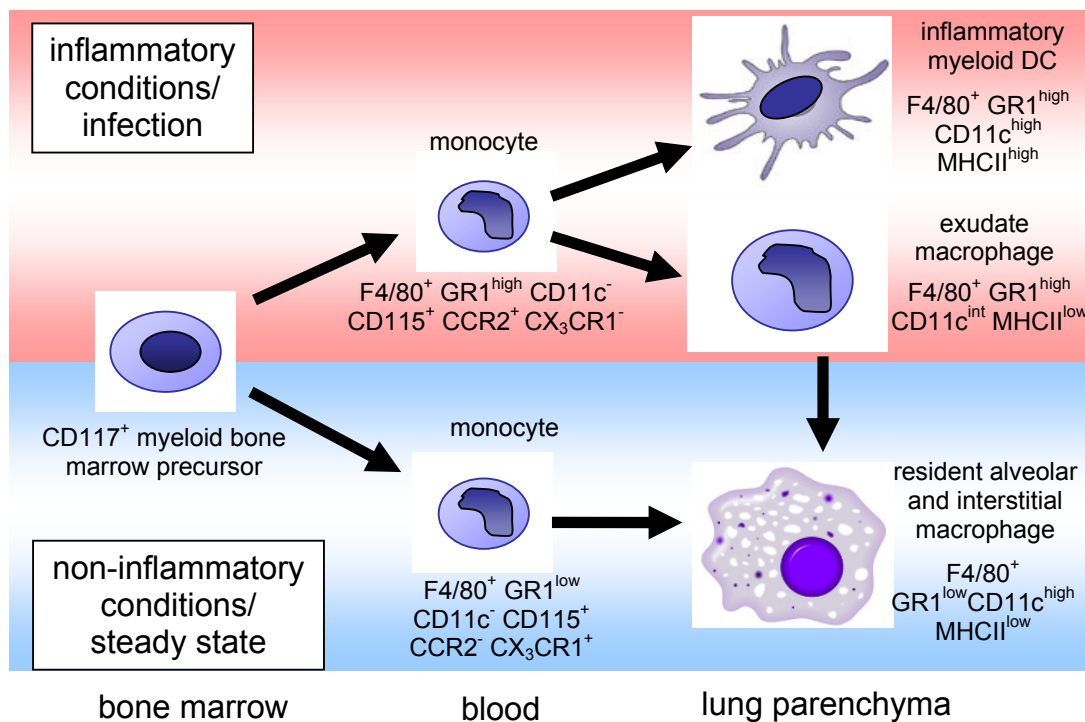
Fig. 2. Murine lung mononuclear phagocytes arise from a common precursor and express distinct surface antigens.

1.4 ARDS and apoptosis

ARDS (adult respiratory distress syndrome) is a severe lung disease caused by a variety of direct and indirect events, the most important being bacterial or viral pneumonia. Recent studies report an annual incidence of up to 200,000 cases per year in the US (48). ARDS is characterized by leukocytic infiltrates and diffuse inflammation of the lung parenchyma leading to alveolar edema and impaired gas exchange with concomitant systemic release of inflammatory mediators frequently resulting in multi-organ failure. Typical histological presentations involve diffuse alveolar damage and hyaline membrane formation in alveolar walls. ARDS is defined by acute onset, bilateral pulmonary infiltrates in the absence of left heart failure and severe hypoxemia. Displaying a mortality rate of 35-40% ARDS usually requires mechanical ventilation (48, 49).

Several authors suggest epithelial cell apoptosis to be an underlying mechanism of alveolar damage in murine and human models of ARDS (50-52). Apoptosis is a form of programmed cell death and involves a series of biochemical processes resulting in cytoplasmic shrinking, loss of cellular polarization, membrane blebbing, nuclear chromatin condensation, and

chromosomal DNA fragmentation (53). The process of apoptosis is controlled by a wide range of cellular signals, which may originate either from an intrinsic or an extrinsic signal, including the TNF-α- and the Fas-Fas ligand (FasL)-mediated pathways. Both of them involve members of the TNF receptor (TNFR) family such as TNFR1, TNFR2, and Fas (CD95). The binding of TNF-α or FasL to their receptors initiates cleavage of cysteine proteases known as caspases via the intermediate membrane proteins TNF receptor-associated death domain (TRADD) and Fas-associated death domain protein (FADD) resulting in the formation of the death-inducing signaling complex (DISC). Both pathways lead to the organised degradation of cellular organelles by activated proteolytic caspases (54)(Fig. 3).

Recently, a further member of the proapoptotic TNF superfamily, tumor necrosis factor (TNF)-related apoptosis–inducing ligand (TRAIL), has been attributed a role in the orchestration of innate and adaptive immune responses (55-57). Being expressed mainly on T cells, NK cells, and mononuclear phagocyte subsets, murine TRAIL exerts its proapoptotic signals in either a membrane-bound or a soluble form via binding to the death receptor 5 (DR5) (45), and displays potent antitumor activity (58-60). Moreover, an antiviral function in experimental murine IV infection has been suggested (57). However, the contribution of TRAIL to alveolar epithelial apoptosis and lung barrier dysfunction during lethal IV pneumonia has not been elucidated yet.
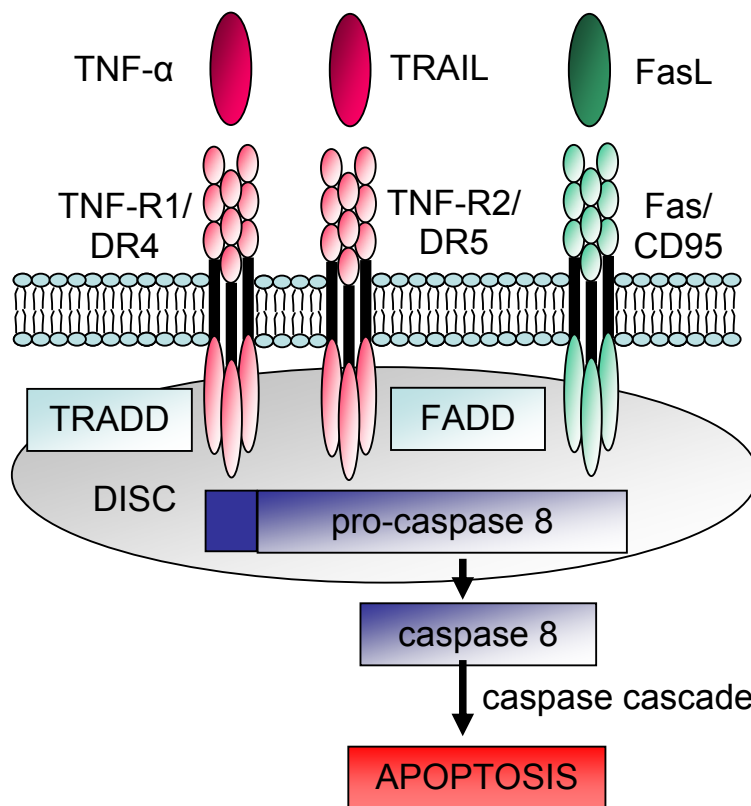
Fig. 3. The extrinsic apoptosis signalling pathway is induced by death ligands TNF-α, TRAIL, and FasL. Upon binding to death receptors, TRADD (TNFreceptor-associated death domain) or FADD (Fas-associated death domain) proteins are recruited to the cytosolic receptor domains and, together with pro-caspase 8, form the death inducing signalling complex (DISC) thereby initiating the caspase cleavage cascade which finally results in apoptosis of the cell.

In the presented thesis, the following questions have been addressed:

1) Which chemokine-receptor interactions mediate monocyte transepithelial migration across IV-infected alveolar epithelial cells *in vitro*?

2) By which pathways are peripheral blood monocytes recruited to the lungs of IV-infected mice *in vivo*?

3) Do exudate macrophages contribute to alveolar epithelial cell apoptosis and lung edema, and if so, which are the molecular interactions involved?

To answer these questions, an *in vitro* model of monocyte transmigration across influenza A virus infected murine primary alveolar epithelial cells was established. Moreover, by the use of the mouse-adapted influenza virus A/PR/8/34 being highly pathogenic in mice, a murine *in vivo* model of IV-

induced acute lung injury was set up to evaluate the recruitment pathways of peripheral blood monocytes into the lung. In addition, the contribution of lung exudate macrophages to alveolar epithelial cell apoptosis and lung barrier dysfunction, and the molecular mediators involved, were analysed in this model.

2. Materials and Methods

2.1 Mice

BALB/c (wildtype) mice, CCR2-deficient mice (BALB/c background), CCR5-deficient mice (B6;129P2-Ccr5^{tm1Kuz}/J) and wildtype mice of the corresponding genetic background (B6129PF2/J) served as donors for alveolar epithelial cells and peripheral blood monocytes used for *in vitro* studies. For *in vivo* infection experiments, C57/BL6 wildtype and CCR2-deficient mice (C57/BL6 background) provided by W.A. Kuziel with a body weight of 18 – 21g were used. Furthermore, we made use of B6.SJL-*Ptprc^a* mice expressing the CD45.1 alloantigen (Ly5.1 PTP) on circulating leukocytes (C57/BL6 genetic background) for bone marrow transplantation experiments. Mice were bred under specific pathogen-free (SPF) conditions. All experiments were approved by our local government committee of Giessen.

2.2 Isolation and culture of murine primary alveolar epithelial cells

Isolation of primary alveolar epithelial cells was performed as described by Corti et al. (61). Mice were killed by an overdose of isoflurane and exsanguinated by cutting the inferior vena cava. After opening the thorax, a small incision was made in the left ventricle, a 26-gauge cannula was placed into the right ventricle and lungs were perfused with 20ml HBSS until they were visually free of blood. A small cut was made into the exposed trachea to insert a shortened 21-gauge cannula that was firmly fixed and a total volume of 1.5 ml of sterile Dispase followed by 500 µl of sterile 1% low-melting agarose in PBS-/- was administered into the lungs. After 2 min of incubation, the lungs were removed and placed into a culture tube containing 2ml of Dispase for 40 min. Lungs were then transferred into a culture dish containing DMEM/2,5%HEPES buffer/0.01% DNAse and the tissue was carefully dissected from the airways and large vessels. The cell suspension was successively filtered, resuspended in 10ml of DMEM supplemented with 10% FCS and antibiotics and incubated with biotinylated rat-anti-mouse CD16/32 and rat-anti-mouse CD45 mAbs for 30 min at 37°C. Cells were then washed and incubated with Streptavidin-linked MagneSphere® Paramagnetic Particles for 30 min at room temperature with gentle rocking followed by magnetic separation of contaminating leukocytes for

15 min. The purity of freshly isolated AEC contained in the supernatant was always >90%, as assessed by pro-SPC immunofluorescence staining specific for type II AEC as well as immunohistochemistry for cytokeratin. Viability was always >95%, as analysed by trypan blue dye exclusion. For cytokine and real time RT-PCR analysis, AEC were plated into 24-well cell culture plates at a density of 5 x 10^5 cells/well and grown to 90% confluence for 5 days in DMEM supplemented with 10% FCS and antibiotics, thereby acquiring a type I alveolar epithelial cell phenotype, as verified by loss of pro-SPC staining. For transmigration assays, 3 x 10^5 AEC were seeded onto the lower side of transwell filter inserts (6.4 mm diameter, 8 µm pore size) and grown for 5 days until they reached 100% confluence.

2.3 Isolation of peripheral blood monocytes

For isolation of peripheral blood monocytes (PB-Mo), mice were sacrificed by an overdose of isoflurane and blood was drawn via the V. cava inferior, transferred into sterile EDTA tubes and diluted with 3ml of PBS-/-. Whole blood cells were carefully layered over 3ml Lympholyte®. Cells were centrifuged at 1400 rpm at room temperature for 35 min to separate the mononuclear fraction. The interphase was collected and mononuclear cells were washed twice in RPMI 1640 supplemented with 10% FCS and antibiotics (10 min, 1200 rpm, RT). Monocytes were further enriched by depleting lymphocytes and CD8-positive NK cells by MACS negative selection using anti-mouse CD4, anti-mouse CD8 and anti-mouse CD19 mAbs, resulting in a final purity of >90%, as assessed by differential counts on Pappenheim-stained cytocentrifuge preparations. Viability of PB-Mo was analysed by trypan blue dye exclusion and was always >95%.

2.4 Virus strain and *in vitro* infection of AEC

Influenza A virus strain A/PR/8/34 (H1N1; PR/8) was grown in the allantoic cavity of embryonated hen eggs. Virus titer was determined by plaque assay on confluent Madin Darby canine kidney cells (see below). AEC cultured on transwells or 24-well plates were washed with PBS-/- and infected with influenza A virus at a MOI of 1 (unless otherwise indicated) in a total volume of 100 µl PBS/BA containing 0.2% bovine serum albumin, 1mM $MgCl_2$, 0.9mM $CaCl_2$, 100U penicillin/ml and 0.1mg streptomycin/ml or with diluent alone

(mock-infection) for 1 h at room temperature. Subsequently, the inoculum was removed and cells were incubated with DMEM supplemented with 2% FCS and 2 µg/ml trypsin (PAA) at 37°C for the indicated time periods.

2.5 Monocyte transmigration assay

For transepithelial migration assays, virus- or mock-infected AEC grown on transwells were incubated in 500 µl DMEM supplemented with 2% FCS and antibiotics added to the lower compartment of 24-well ultra low cluster plates for 32 h. In some experiments, recombinant murine CCL2 or CCL5 were added to the medium of non-infected AEC. 4 x 10^5 PB-Mo in 100µl RPMI/10% FCS were then added into transwell inserts to allow their transmigration through AEC in a basal towards apical orientation of the epithelial monolayer for 90 min at 37°C. Transmigrated monocytes were collected from the lower chamber with 200µl aliquots of ice-cold 5 mM EDTA in PBS-/-, then centrifuged and resuspended in 50µl RPMI and total cell numbers were counted in a hemocytometer. In selected experiments, neutralizing anti-CCL2 mAb (1µg/ml) was added to the medium of each well at 6, 12, and 20 h after infection.

2.6 Cytokine quantification

Cytokine levels in the supernatants of infected AEC or in bronchoalveolar lavage fluid (BALF; see below) were measured using commercially available colorimetric sandwich ELISA kits. Standards were prepared by serial 1:10 dilutions with assay diluent. Standards, samples and positive controls were added to the antibody-coated plate in duplicates and incubated for 2 h at RT. Plates were washed five times with 400µl of washing buffer with an ELISA autowasher. After incubation with 100µl of conjugate solution per well for 2 h and additional washing steps, 100µl of substrate solution was added for 30min and the reaction was stopped. Optical density was measured using a microplate reader set to 450nm. Detection limits were 2 pg/ml for CCL2 and CCL5, and 5.1 pg/ml for TNF-α.

2.7 *In vivo* infection and mouse treatment protocols
2.7.1 Intratracheal infection with influenza virus PR/8

Mice were anesthetized with xylazine hydrochloride (2.5mg/kg im) and ketamine hydrochloride (50mg/kg im), and the neck fur above the trachea was shaved followed by desinfection of the skin. A small incision was made, and the underlying connective tissue was bluntly dissected to expose the trachea. A 26-gauge Abbocath was inserted into the trachea, and mice were slowly inoculated with 500PFU of influenza virus PR/8 diluted in sterile PBS-/- in a total volume of 70µl or mock-infected with PBS-/- alone. Subsequently, the catheter was removed, and the skin was sutured. Mice were allowed to recover from anesthesia and were then returned to their cages, with free access to food and water. In some experiments, mice were anesthetized as described above and azide-free function-blocking mAbs (75µg anti-CCR2 (29) in 100µl PBS-/- at d0 and d4 pi or 150µg anti-TRAIL (N2B2) in 150µl PBS-/- at d3 and d5 or at d3, d5, d7, and d9) or respective isotype IgG control antibodies were injected intraperitoneally. For body weight and survival analysis PR/8 infected mice were observed and weighed every 24 h pi for 21 days.

2.7.2 Bronchoalveolar lavage

At the indicated time points, mice were sacrificed by an overdose of isoflurane and bronchoalveolar lavage (BAL) was performed as follows: After exposure of the trachea, a small incision was made to insert a shortened 21-gauge cannula that was firmly fixed and then connected to a 1ml syringe filled with 300µl of PBS-/-/5mM EDTA (pH 7.2). BAL was performed with 300µl aliquots until an initial BAL volume of 1.5ml was recovered. The cells were separated by centrifugation (10 min, 1200rpm, 4°C), and the supernatant was used for quantification of CCL2 and TNF-α protein or for the lung permeability assay (see below). Subsequently, BAL was completed with 500µl aliquots until an additional BAL volume of 4.5ml was recovered. BAL cells from the first and second BAL fraction were pooled, counted with a hemacytometer and differential cell counts of Pappenheim-stained cytocentrifuge preparations were performed using overall morphological criteria, including differences in cell size and shape of nuclei. For flow cytometric analysis, BAL leukocytes were fixed in ice-cold PBS-/-/1%PFA for 15 min, washed and resuspended in FACS buffer (PBS-/- supplemented with 7.4 % (v/v) EDTA and 0.5 % (v/v) FCS).

2.7.3 Isolation of peripheral blood leukocytes

For isolation of peripheral blood leukocytes mice were sacrificed at the indicated time points and the abdominal cavity was rapidly opened to expose the vena cava. Blood was drawn into a 23-gauge cannula connected to a 1-ml insulin syringe that was filled with 200µl of NaCl-EDTA as an anticoagulant. Blood samples were hemolysed in a total volume of 10 ml of an ammonium chloride solution (pH 7.2) for 3 min and leukocytes were resuspended in RPMI/10%FCS, washed (10 min, 1200rpm, RT), and after a second hemolysis step fixed in ice-cold PBS-/-/1%PFA for 15 min before resuspension in FACS buffer for further flow cytometric analysis.

2.8 Preparation of lung homogenates

PR/8 or mock infected mice were sacrificed at the indicated time points and exsanguinated by cutting the V. cava inferior. After opening the thorax, a small incision was made in the left ventricle, a 26-gauge cannula was placed into the right ventricle and lungs were perfused with 20ml HBSS until they were visually free of blood. 1.5ml of Dispase followed by 500µl of 1% low-melting agarose in PBS-/- were administered into the lungs via the trachea through a firmly fixed 21-gauge cannula. After 2 min of incubation, the lungs were dissected out of the thorax and put into a culture tube containing 2ml of Dispase for 40 min at RT. Lungs were then transferred into a culture dish containing DMEM/2,5%HEPES buffer and 0.01% DNAse and the tissue was carefully dissected from the airways and large vessels with forceps and sheared through a 1ml pipet tip. The cell suspension was successively filtered through 100µm- and 40µm-filters, washed twice in DMEM/10%FCS and resuspended in Annexin V staining buffer (10 mM HEPES, 140 mM NaCl, and 2.5 mM $CaCl_2$) or FACS buffer for flow cytometric analysis.

2.9 Lung permeability assay

For the determination of alveolar leakage mice received an intravenous injection of 1mg FITC-labelled albumin in 100µl of sterile NaCl 0.9%. 45 min later, BALF and blood samples were collected as described above. Blood samples were incubated for 3 h at RT without addition of EDTA until coagulation occurred and serum was recovered after centrifugation (3500rpm, 15 min, RT). FITC

fluorescence was measured in duplicates in undiluted BALF and serum samples (diluted 1:100 in PBS-/-) and compared to standard samples serially diluted 1:10 with PBS-/- using a fluorescence spectrometer. The lung permeability index is defined as the ratio of fluorescence signals of undiluted BALF samples to fluorescence signals of 1:100 diluted serum samples and given as arbitrary units (AU).

2.10 Quantification of lung virus titers

Lungs from PR/8 infected mice were dissected out of the thorax and heart and connective tissue were removed. Lungs were mechanically homogenized in 2ml PBS+/+ in glass douncers on ice, centrifuged at 4000rpm for 10 min at 4°C and supernatants were serially diluted ($1:10^0$ to $1:10^7$) in PBS/BA. Virus titers were determined by immunohistochemistry on confluent Madin Darby canine kidney cells in 96-well plates in duplicates. Cells were incubated with 50µl of homogenate dilution for 1 h at room temperature and after removal of the inoculum covered with 1.5% methylcellulose media containing 2µg/ml trypsin for 72 h. Cells were permeabilised and fixed with PBS+/+/4%PFA/1%Triton X-100, washed three times with 400µl of Tween buffer (0.2% Tween 20 in PBS-/-) and incubated with diluted primary mouse anti-IV nucleoprotein-mAb for 45 min at RT. After three washing steps, diluted HRP-conjugated anti-mouse IgG was added for 45 min. After additional washing steps, the peroxidase substrate AEC (3-amino-9-ethylcarbazole) was added for 10 min. Foci were counted using a Leica light microscope and are given as foci forming units (FFU) per lung.

2.11 Flow cytometry and cell sorting

Flow cytometric analysis was performed using a FACSCanto flow cytometer (BD Biosciences) equipped with a FACSDiva Software package.

2.11.1 Chemokine receptor analysis on isolated PB-Mo

Chemokine receptor analysis on isolated PB-Mo was performed as follows: Cells were washed and incubated for 40 min at 4°C with rat anti-mouse CCR5 (MC68), rat anti-mouse CCR2 (MC21), both provided by M. Mack (29), or rat IgG isotype antibodies, all diluted to working concentrations. Unspecific antibody binding was inhibited by adding 10µl Fc-Block. Cells were then

washed twice with FACS buffer and incubated with PE-labelled goat anti-rat IgG for 20 min at 4°C. After two further washing steps, CCR2 and CCR5 expression were analysed in the PE-channel.

2.11.2 Analysis of leukocyte subpopulations in BAL from PR/8 infected mice

For flow cytometric analysis of fixed blood or BAL leukocytes from *in vivo* experiments 5×10^5 cells were washed in FACS buffer. Unspecific antibody binding was inhibited by adding 10µl Fc-Block. Cells were stained with biotinylated or fluorochrome-labeled primary mAbs and analysed either for "myeloid" cell composition (CD45.2-FITC (30F-11), GR1-PE (RB6-8C5), biotinylated I-A/I-E (2G9), F4/80-Alexa647 (CI:A3-1), CD11c-PE-Cy5.5 (418)) or for lymphocyte subpopulations (CD45.2-PerCP-Cy5.5 (30F-11), NK1.1-APC (PK136), CD4-FITC (RM4-4), biotinylated CD8α (53-6.7)). Antibodies were diluted to working concentrations and added for 20 min. After 2 washing steps with FACS buffer (3 min, 1200rpm, 4°C), biotinylated primary mAbs were further incubated with 5µl of 1:100 diluted APC-Cy7-conjugated streptavidin for 5 min and 5-colour flow cytometry was performed. Data from the myeloid cell analysis is given as dot plots and represent a three-hierarchy gating. CD45$^+$ cells (P1, leukocytes) were gated according to their GR1- and F4/80-expression. GR1^{int}F4/80$^+$ cells represent alveolar mononuclear phagocytes (P2). Subgate analysis of P2 revealed a CD11c^{int} (P3, exudate macrophages), and a CD11c^{high} (P4, resident AM) subpopulation, as well as a CD11c^{high}MHCII^{high} subpopulation (P5) representing alveolar dendritic cells. Lymphocyte subpopulation analysis (NK-cells, CD4 T-cells, CD8 T-cells) was performed by gating on CD45-positive cells and their relative proportion was calculated according to their NK1.1-, CD4-, and CD8a-expression, respectively.

2.11.3 Analysis of bone marrow transplantation efficiency

For analysis of bone marrow engraftment efficiency in chimeric mice (see below), fixed BAL and blood cells were stained with anti-mouse CD45.2-FITC (30F-11) and CD45.1-PE (A20) mAbs for 20 min and the relative proportions of donor (CD45.2) and recipient (CD45.1) leukocytes in blood and of resident AM in BAL was calculated.

2.11.4 Quantification of alveolar type I epithelial cell apoptosis from PR/8 infected lung homogenates

Epithelial apoptosis in lung homogenates was analysed by quantitation of annexin V binding. 1×10^6 cells were washed in annexin V staining buffer. Unspecific antibody binding was inhibited by adding 10µl Fc-Block. Cells were stained with PE-labelled anti-mouse CD45.2 (30F-11) mAb, hamster anti-mouse T1α mAb and annexin V-Alexa647 conjugate, each diluted to working concentrations, for 20 min. After two washing steps, cells were further incubated with Alexa 488-labelled anti-hamster Ig secondary antibody for 20 min. CD45-negative cells were gated and analysed for their T1α expression (FITC-channel) and annexin V binding (APC-channel).

2.11.5 Quantification of TRAIL expression on BAL leukocytes

Analysis of TRAIL expression on BAL leukocytes was performed as described above with either a combination of GR1-FITC (RB6-8C5), F4/80-Alexa647 (CI:A3-1), and TRAIL-PE (N2B2, or rat isotype-PE IgG) anti-mouse mAbs or a combination of NK1.1-APC (PK136), CD4-FITC (RM4-4), biotinylated CD8α (53-6.7) and TRAIL-PE (N2B2, or rat isotype-PE IgG) anti-mouse mAbs followed by further incubation with 5µl of 1:100 diluted APC-Cy7-conjugated streptavidin for 5 min. TRAIL expression on mononuclear phagocytes ($GR1^{int}F4/80^+$), neutophils ($GR1^{int}F4/80^+$), NK-cells ($SSC^{low}NK1.1^+$), CD4 T cells ($SSC^{low}CD4^+$), and CD8 T cells ($SSC^{low}CD8a^+$) was quantified.

2.11.6 DIVA-assisted high speed sorting of PB-Mo and exudate macrophages

For cell sorting experiments, unfixed BAL cells pooled from 8 mice per experiment were incubated with GR1-PE-Cy7 (RB6-8C5), F4/80-Alexa488 (BM8), and CD11c-PE (HL3) anti-mouse mAbs for 20 min. Unfixed blood leukocytes from the same animals or from mock-infected mice were pooled and stained with anti-mouse CD11b-FITC (M1/70) and CD115-PE (MCA1898) mAbs for 20 min. $F4/80^+GR1^{int}CD11c^{int}$ BAL cells (exudate macrophages) and $SSC^{low}CD11b^{high}CD115^{high}$ blood cells (PB-Mo) were high-purity sorted with a FACSVantage SE flow cytometer equipped with a DIVA sort option, an argon-ion laser operating at 488 nm excitation wavelength and a HeNe laser operating at 633 nm excitation wavelength. The BD FACSDIVA software package was

used for data analysis. After cell sorting, the purity of the cell preparations was analyzed by *1*) postsort analysis of sorted cells and *2*) differential cell counts of Pappenheim-stained sorted cells. The cell purity of sorted peripheral blood monocytes and exudate alveolar macrophages was always >90%.

2.11.7 Quantification of DR5 expression on PR/8 infected alveolar type I epithelial cells from lung homogenates

1×10^6 lung homogenate cells were prepared as described in chapter 2.8 and fixed for 15 min in PBS/1%PFA before resuspension in FACS buffer, permeabilized with 0.2% saponin and unspecific antibody binding was inhibited by adding 10µl Fc-Block. Cells were stained with PE-labelled anti-mouse CD45.2-PE-Cy5.5 (30F-11) mAb, hamster anti-mouse T1α mAb, mouse anti-influenza nucleoprotein mAb (clone 1331), and rat anti-mouse DR5 (TNFR2) mAb or rat isotype IgG control, each diluted to working concentrations, for 20 min. After two washing steps, cells were further incubated with Alexa 488-labelled anti-hamster Ig, Alexa 647-labelled anti-mouse Ig, and PE-labelled anti-rat Ig secondary antibodies for 20 min. CD45-negative/T1α-positive cells were gated and analysed for their nucleoprotein and DR5 expression.

2.12 Generation of bone marrow chimeric mice

Bone marrow cells were isolated under sterile conditions from the tibias and femurs of wildtype C57/BL6 or from CCR2$^{-/-}$ donor mice. The proximal and distal ends of donor tibias and femurs were cut with a scalpel and flushed with sterile RPMI/10% FCS. A bone marrow single cell suspension was prepared, filtered through 70 µm and 40 µm nylon meshes and cell suspensions were then washed in Leibovitz L15 medium prior to transplantation. Recipient wildtype C57/BL6 mice received 6 Gy of lethal body irradiation. A total of 1.2×10^7 wildtype or CCR2$^{-/-}$ donor bone marrow cells were transplanted via intravenous injection into the tail vein of sedated wildtype recipient mice. For some experiments, wildtype and CCR2$^{-/-}$ bone marrow cells were mixed at a 1:1 ratio prior to transplantation. As controls for bone marrow engraftment, wildtype C57/BL6 bone marrow cells (expressing the CD45.2 alloantigen) were transplanted into CD45.1 alloantigen-expressing mice (n=2 during each transplantation experiment) and the proportion of CD45.2 positive peripheral

blood and BAL leukocytes was analysed by flow cytometry as described above. Bone marrow engraftment was 90.5 ± 2.7% after two weeks post transplantation. Chimeric mice were housed under SPF conditions for 14d prior to PR/8 infection.

2.13 Preparation of lung tissue sections and TUNEL assay

HBSS-perfused lungs were carefully lavaged with 400µl aliquots of PBS-/-/2mM EDTA to wash out alveolar leukocytes and thereafter slowly inflated with 1,5ml of a 1:1 mixture of TissueTek OCT and PBS-/-, removed en bloc and snap-frozen in liquid nitrogen. Lung tissue cryosections were mounted on glass slides and dried overnight at room temperature. Apoptotic cells were stained using the DeadEnd® Colorimetric TUNEL system. Sections were fixed in PBS-/-/4%PFA, washed and permeabilized with Proteinase K solution. Fragmentated DNA was labeled by incorporation of biotinylated nucleotides at the 3`-OH-ends using deoxynucleotidyl transferase (TdT reaction mix). Thereafter, the reaction was stopped with 2xSSC, washed, and 100µl of Streptavidin-linked HRP were added on the slides. After additional washing steps the sections were developed with 100µl of DAB (3,3'-diaminobenzidine), washed and mounted in aqueous mounting medium. Slides were analysed with a Leica DM 2000 light microscope at the indicated magnification using a Leica digital imaging software.

2.14 RNA isolation and real time RT-PCR

Flow-sorted blood monocytes and exudate macrophages were lysed with RLT buffer containing ß-mercaptoethanol and RNA was isolated with spin columns using the RNeasy Micro Kit, whereas RNA from cultured alveolar epithelial cells was isolated by PeqGold Total RNA kit. For cDNA synthesis, 2-500ng of denatured template was added to a mastermix containing 5µl 5x1st strand buffer, 2.5µl DDT, 0.5µl Rnase inhibitor, 1µl 10mM DNTPs, 1.5µl Random Hexamers, 0.25µl dH$_2$O, and 0.75µl MMLV-Reverse Transcriptase per reaction, incubated for 50 min on 37°C and the reaction was stopped by heating to 96°C for 5 min in a PE GeneAmp PCR System 2400. For analysis of quantitative mRNA expression PBGD was used as the reference gene. Reactions were performed in an ABI 7900 Sequence Detection System using SYBR-Green I as

fluorogenic probe in 25µl reactions containing 5µl cDNA sample, 1× Platinum SYBR® Green qPCR SuperMix and 45 pmol forward and reverse primers. The following primer sequences were used:

TNF-α: FP: 5'- CAT CTT CTC AAA ATT CGA GTG ACA A-3',

               RP: 5'- TGG GAG TAG ACA AGG TAC AAC CC-3';

FasL: FP: 5'-CCA ACC AAA GCC TTA AAG TAT CAT C-3',

               RP: 5'- AAC CCA GTT TCG TTG ATC ACA A-3';

TRAIL: FP: 5'- GAA GAC CTC AGA AAG TGG C -3',

               RP: 5' – GAC CAG CTC TCC ATT CCT A-3';

DR5:   FP: 5'- AAG TGT GTC TCC AAA ACG G-3',

               RP: 5' – AAT GCA CAG AGT TCG CAC T – 3';

PBGD: FP: 5' – GGT ACA AGG CTT TCA GCA TCG -3',

               RP: 5' – ATG TCC GGT AAC GGC GGC -3'.

Relative expression was determined by the $2^{\Delta\Delta Ct}$ method.

2.15 Statistical analysis

All data are given as mean ± SD. For analysis of statistical differences, one-factor ANOVA with posthoc test by Dunnett or Student´s t-test were applied. Statistical significances between treatment groups were calculated with the SPSS for Windows software program. Significance was assumed when *p* values were ≤ 0.05.

3. Results

3.1 PR/8 infection of AEC promotes monocyte transepithelial migration

To investigate whether PR/8 infection of AEC provokes a basal-to-apical monocyte transepithelial migration, isolated peripheral blood monocytes were added to transwell filter inserts containing either PR/8 or mock-infected AEC. Transmigration rates were compared to monocyte migration across mock-infected AEC driven by recombinant CCL2 or CCL5 that was added to the lower transwell compartment. Monocyte transmigration across PR/8 infected AEC monolayers was increased 10-fold compared to transmigration across mock-infected AEC, indicating that PR/8 infection of AEC strongly induced monocyte recruitment across the infected epithelial cell barrier. Monocyte transmigration across PR/8 infected AEC even exceeded monocyte migration across mock-infected AEC driven by exogenously added recombinant CCL2 or CCL5 (Fig. 4).
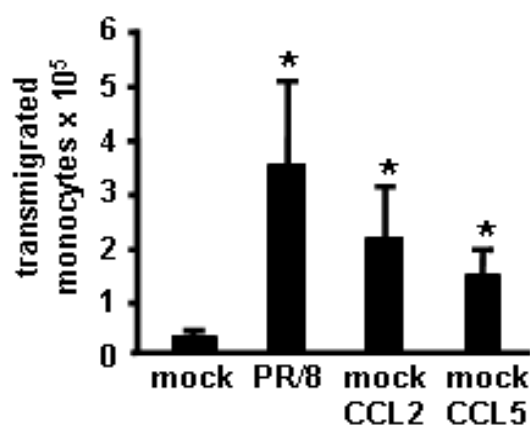
Fig. 4. PR/8 infection of AEC promotes transepithelial migration of peripheral blood monocytes. Monocytes purified from peripheral blood were allowed to transmigrate either mock-infected AEC, PR/8 infected AEC (32 h) or mock-infected AEC in the presence of recombinant CCL2 or CCL5 added to the lower transwell compartment (200 ng/ml) in a basal-to-apical direction for 90 min. Values are presented as mean ± SD from n = 5 experiments; *$p < 0.05$ for comparison with mock-infected AEC.

3.2 Monocyte transmigration induced by epithelial PR/8 infection is dependent on the CCL2/CCR2 axis

To further characterize the chemotactic factors driving *in vitro* monocyte transmigration across PR/8 infected AEC, we evaluated whether PR/8 infection of AEC induced the release of the major monocyte-attracting chemokines, CCL2 and CCL5 into the supernatant. Both CCL2 and CCL5 release was induced in a time- and MOI-dependent manner peaking at 32 h post-infection at a MOI of 1 (Fig. 5). To further evaluate the role of epithelial-derived CCL2 or CCL5 to drive transepithelial monocyte migration, peripheral blood monocytes collected from mice lacking the respective chemokine receptors (CCR2^{-/-} or CCR5^{-/-}) were compared with congenic wild-type monocytes for their transmigration capacity across PR/8 infected AEC. As demonstrated in Fig. 6A, both CCR2 and CCR5 were expressed on wild-type monocytes. Lack of the CCL2 receptor on monocytes collected from CCR2^{-/-} mice resulted in a 90% reduced monocyte transepithelial migration. Moreover, neutralization of epithelial cell-derived CCL2 by addition of CCL2-neutralizing antibodies similarly reduced the monocyte transmigration. In contrast, CCR5-deficient monocytes transmigrated PR/8 infected epithelium to the same extent as wild-type monocytes (Fig. 6B). These data demonstrate a crucial role for the CCL2/CCR2 axis in monocyte migration across influenza A virus infected alveolar epithelial cells.
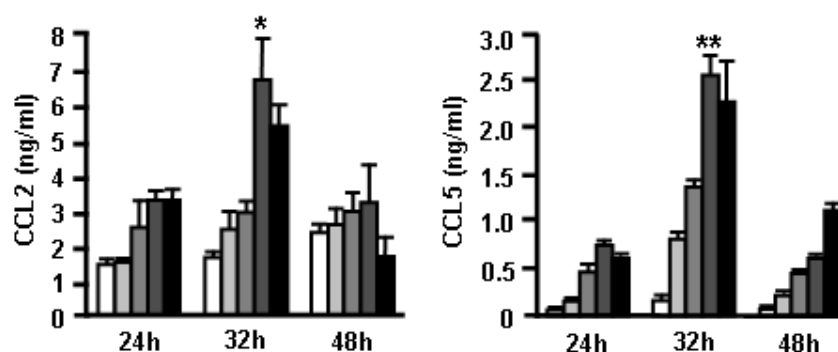

Fig. 5. CCL2 and CCL5 release from PR/8 infected AEC. AEC were mock-infected (white bars) or infected with PR/8 for the given time periods with the following MOIs: 0.1 (light grey bars), 0.5 (medium grey bars), 1 (dark grey bars), or 2 (black bars). Values are presented as mean ± SD (n = 3 for all experiments except at 32 h where n = 4); **$p < 0.01$ and *$p < 0.05$ for comparison with mock-infected AEC of the respective time point.
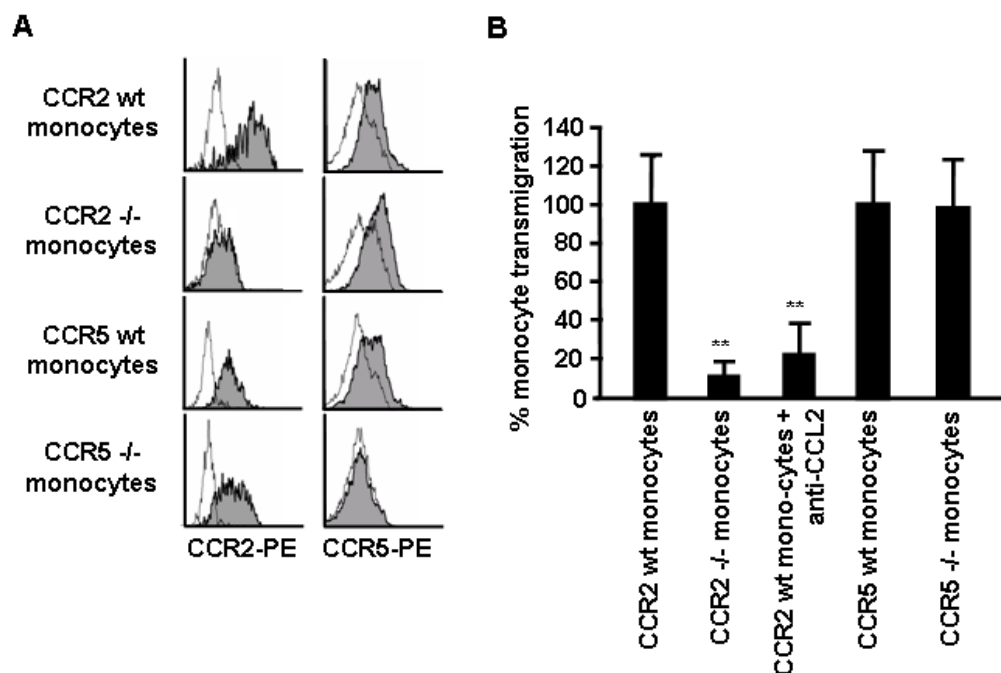
Fig. 6. Monocyte transmigration across PR/8 infected AEC is CCL2/CCR2 dependent. **(A)** Representative FACS histograms of CCR2 (left panel) and CCR5 (right panel) expression on PB-Mo (x-axis, PE-fluorescence; y-axis, total events; white histograms, PE-labeled isotype control; grey histograms, anti-CCR5-PE or anti-CCR2-PE). **(B)** Monocytes derived from CCR2^{-/-} or CCR5^{-/-} mice or from wild-type mice were allowed to transmigrate PR/8 infected AEC isolated from corresponding wild-type mice. Where indicated, neutralizing anti-CCL2 antibodies (1µg/ml) were added to the AEC medium followed by wild-type monocyte transmigration. Values are presented as percent monocyte transmigration calculated from each experiment (mean ± SD of at least 5 independent experiments); **$p < 0.01$.

3.3 CCR2-deficiency selectively affects alveolar mononuclear phagocyte recruitment during IV pneumonia

To evaluate the amount and composition of alveolar leukocyte infiltration in PR/8 infected wildtype and CCR2^{-/-} mice, total BALF cell counts and cell differentials were determined at various time points post infection. No significant differences in total BALF cell counts were detectable between the two treatment groups (Fig. 7).
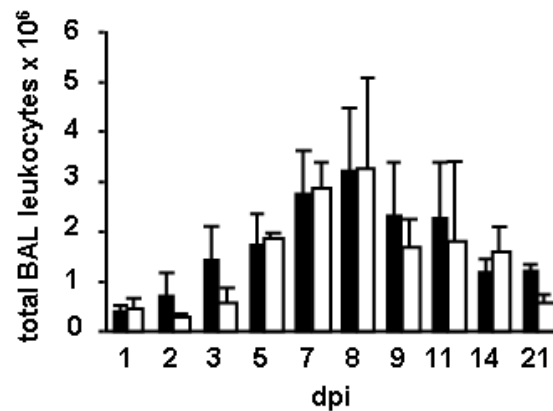
Fig. 7. Quantification of total leukocyte numbers in BALF of PR/8 infected wt (■) or CCR2⁻ ⁄⁻ (□) mice (n=3–5 mice per group, values are given as mean ± SD).

Morphologic analysis of leukocyte composition from Pappenheim-stained BALF cytospin preparations of PR/8 infected wildtype or CCR2$^{-/-}$ mice revealed that peak alveolar neutrophil accumulation was delayed in CCR2-deficient mice but did not significantly differ from peak values reached in wildtype mice (CCR2$^{-/-}$ mice: 73.3 ± 8.0% on day 7 pi; wildtype mice: 63.6 ± 17.8% on day 3 pi), being in line with previous reports (21). Lymphocyte recruitment was virtually identical in both treatment groups as was the reduction of the resident alveolar macrophage proportion in BALF that reflects the pronounced alveolar accumulation of leukocytes in both wildtype and CCR2-deficient mice during the time course of infection. However, alveolar mononuclear phagocyte recruitment was found to be strongly reduced in CCR2-deficient mice, most prominent at day 8 post infection (34.3 ± 7.4% vs. 7.6 ± 6.7%; Fig. 8).

Correspondingly, exudate mononuclear phagocyte numbers were significantly decreased in PR/8 infected wildtype mice pretreated intraperitoneally with an anti-CCR2 antibody by day 8 post infection, as compared to mice treated with isotype control (Fig. 9).
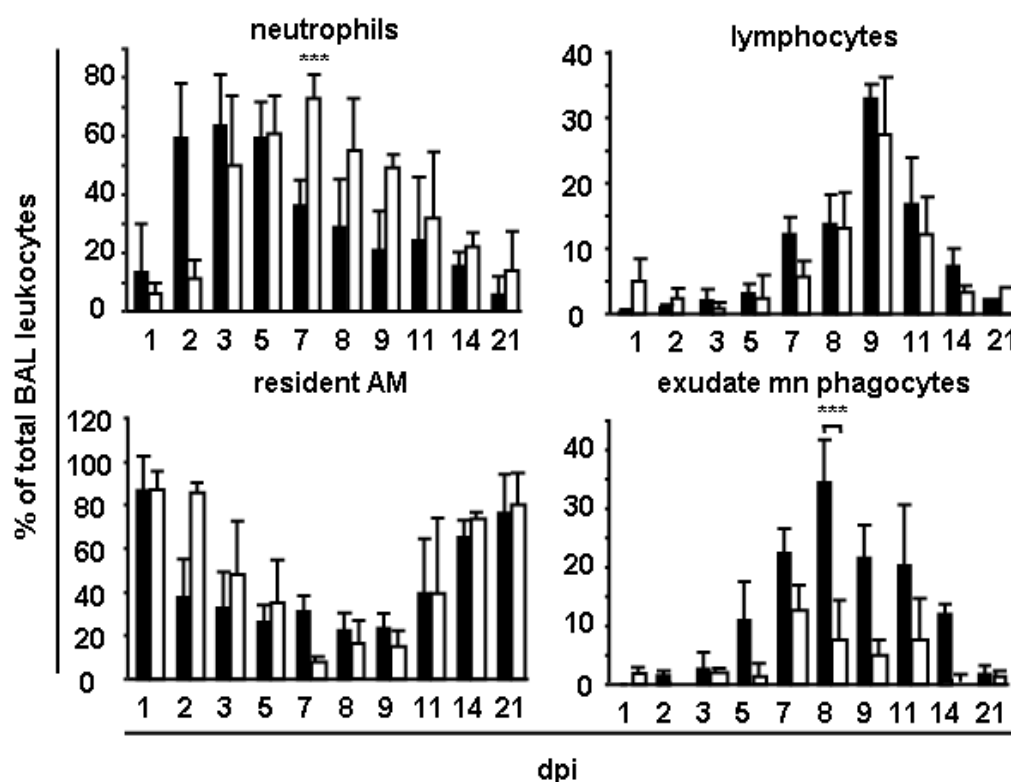
Fig. 8. Quantification of BAL leukocyte subpopulations from Pappenheim-stained cytocentrifuge preparations of PR/8 infected wt (■) or CCR2$^{-/-}$ (□) mice (values are given as mean ± SD of n=3–5 mice per group; *** $p < 0.005$; AM, alveolar macrophages; mn, mononuclear).
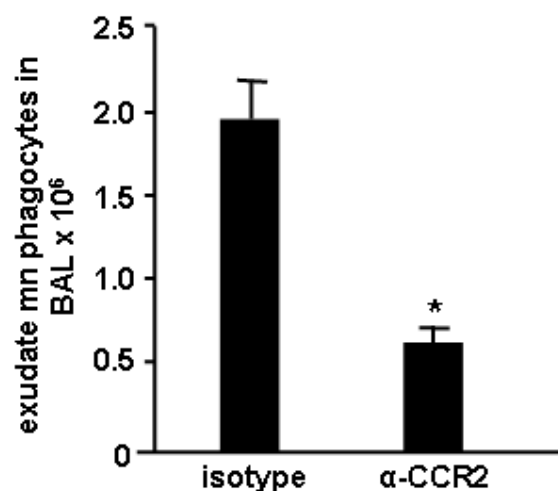

Fig. 9. Quantification of BALF exudate mononuclear phagocytes from PR/8 infected wt mice treated with IgG isotype or anti-CCR2 mAb. Values are calculated from differential counts of BAL leukocytes and are given as mean ± SD of n=5 mice per group; * $p < 0.05$.

To further dissect the alveolar mononuclear phagocyte subset composition, BALF cells gained from PR/8 infected mice of the various treatment groups were subjected to flow cytometric analysis for surface marker expression at day 8 post infection. Analysis of CD45$^+$ BALF cells (leukocytes, P1; Fig. 10, first column) for GR1 and F4/80 expression revealed three distinct cell populations: Gr1^{high}F4/80$^-$ neutrophils, GR1$^-$F4/80$^-$ lymphocytes, and GR1^{int}F4/80$^+$ mononuclear phagocytes (P2; Fig. 10, second column), which were composed of a CD11c^{int} (P3, henceforth termed "exudate macrophages") and a CD11c^{high} (P4) subpopulation, representing resident alveolar macrophages, according to previous reports (40, 41). Exudate macrophages (P3) accumulated to a much lesser extent in CCR2$^{-/-}$ mice or in mice pretreated with anti-CCR2 antibodies as compared to wildtype mice or isotype-treated mice, respectively (Fig. 10, third column). Alveolar mononuclear phagocytes (P2) contained a low proportion of dendritic cells (CD11c$^+$MHCII^{high}, P5; Fig. 10, fourth column).
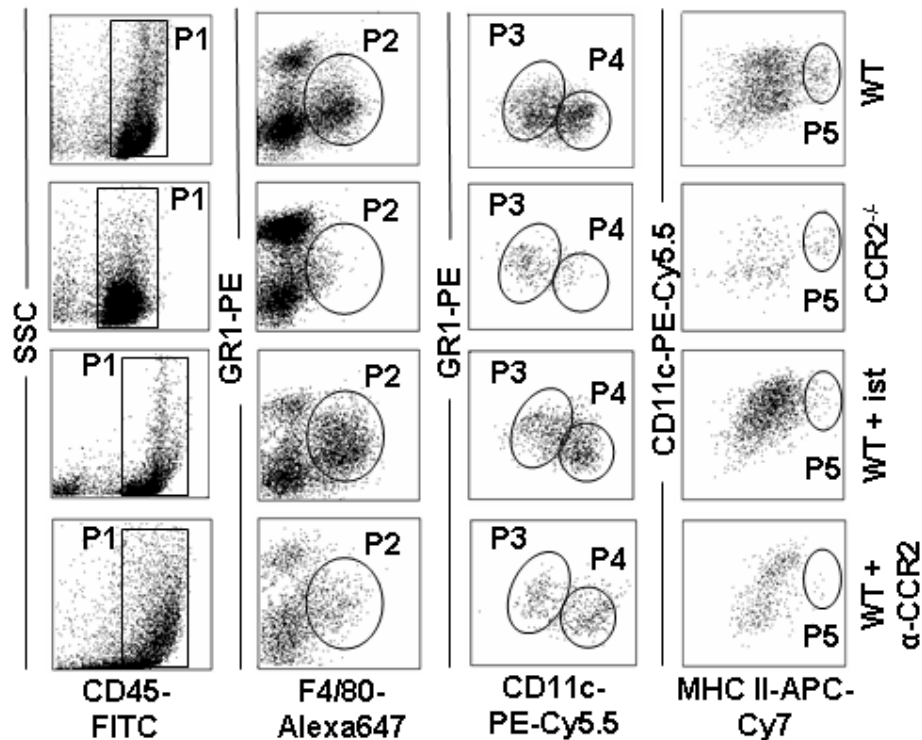
Fig. 10. **Flow cytometric analysis of alveolar mononuclear phagocyte subpopulations in PR/8 infected wt versus CCR2$^{-/-}$ mice or in wt mice treated with IgG isotype or anti-CCR2 mAb** was performed by three-hierarchy gating on d8 pi. CD45$^+$ cells (P1) were gated according to their GR1- and F4/80-expression. GR1^{int}F4/80$^+$ cells represent alveolar mononuclear phagocytes (P2). Subgate analysis of P2 revealed a CD11c^{int} (P3, exudate macrophages), and a CD11c^{high} (P4, resident AM) subpopulation, as well as a CD11c^{high}MHCII^{high} subpopulation (P5) representing alveolar dendritic cells; ist, isotype control.

Flow cytometric quantification of alveolar dendritic cell accumulation or lymphocyte subset recruitment was performed in wildtype and CCR2-deficient mice on various time points post PR/8 infection. Alveolar dendritic cell recruitment was delayed in PR/8 infected CCR2$^{-/-}$ mice but reached peak values comparable to wildtype mice by day 8 post infection (Fig. 11, left panel). Flow cytometric analysis of alveolar lymphocyte subsets revealed no striking differences in the recruitment of NK cells, CD4$^+$ T cells or CD8$^+$ T cells between wildtype and CCR2-deficient mice at the given time points (Fig. 11).
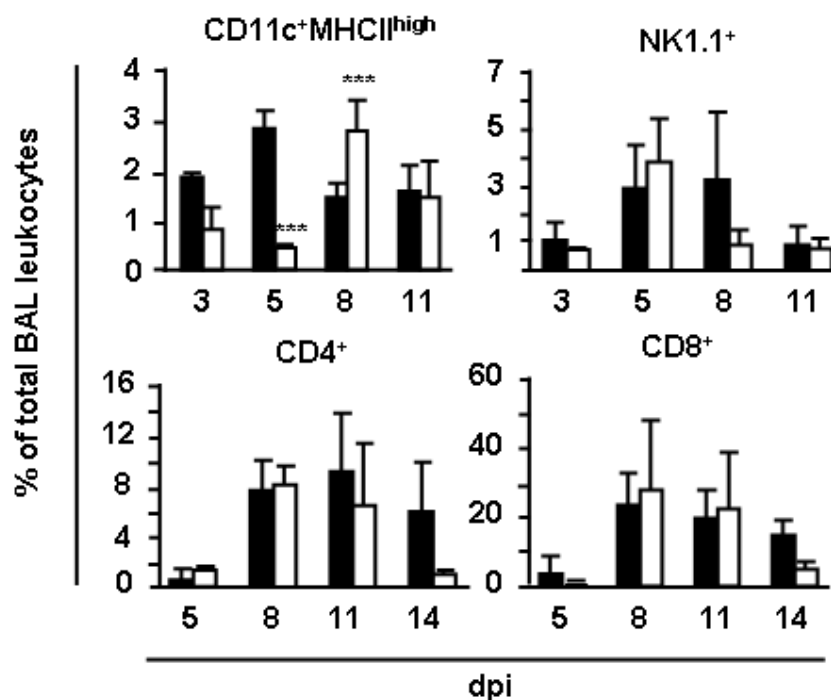
Fig. 11. Flow cytometric quantification of CD11c^{high}MHCII^{high} dendritic cells (left panel) and lymphocyte subpopulations from BAL leukocytes of PR/8 infected wt (■) versus CCR2^{-/-} (□) mice (using the gating characteristics described in Fig. 7 for dendritic cells). For analysis of lymphocyte subpopulations, CD45^{+} cells were subgated on NK cells (SSC^{low}NK1.1^{+}), CD4 T cells (SSC^{low}CD4^{+}), and CD8 T cells (SSC^{low}CD8^{+}). Data is given as percent of CD45^{+} cells; n=3-5 mice per experiment; *** $p < 0.005$; SSC, side scatter.

As shown in Fig. 12, quantification of the primary CCR2 ligand, CCL2, in BAL fluid revealed a pronounced alveolar CCL2 release upon PR/8 infection in both wildtype and CCR2-deficient mice, with CCL2 secretion being even > 10-fold higher in CCR2^{-/-} mice at day 5 post infection, an effect which has been described previously (62).

Altogether, corresponding to the *in vitro* findings, the presented data demonstrate that accumulation of GR1^{int}F4/80^{+}CD11c^{int}MHCII^{low} exudate macrophages in the alveolar air space during PR/8 pneumonia was severely impaired in CCR2-deficient mice or wildtype animals treated with function blocking anti-CCR2 antibodies, demonstrating a key role of the CCL2/CCR2-axis during IV-induced lung macrophage recruitment *in vivo*.
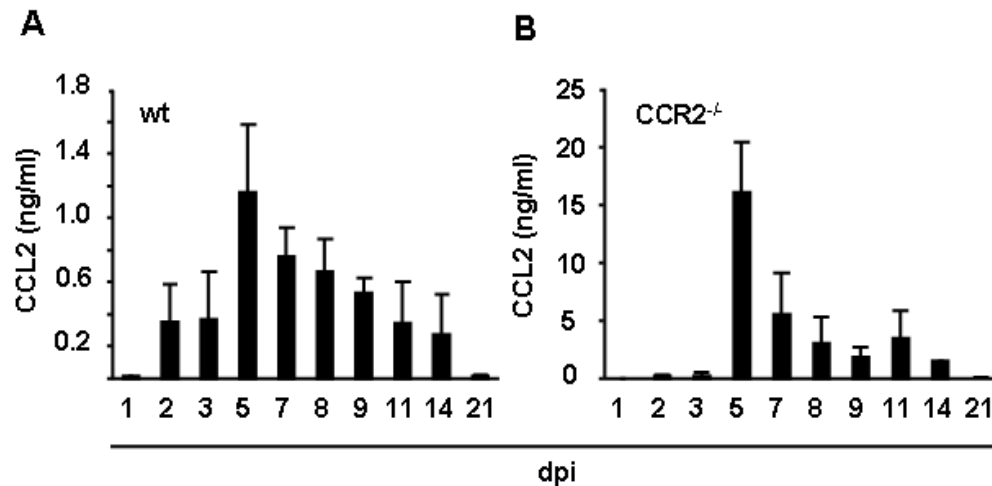
Fig. 12. Quantification of CCL2 levels in BALF from PR/8 infected wt and CCR2$^{-/-}$ mice. Mice were inoculated with PR/8 and BAL was performed at the indicated time point post infection prior to CCL2 protein quantification by ELISA (values depict means ± SD of n=3-5 mice per time point).

3.4 Genetic deletion of CCR2 reduces mortality, morbidity, and alveolar barrier dysfunction during PR/8 infection

To investigate whether exudate macrophage recruitment to the lungs of IV-infected mice might affect the outcome of IV pneumonia, wildtype and CCR2$^{-/-}$ mice were intratracheally inoculated with PR/8 and survival and body weight were determined during 21 days post infection. As shown in Figure 13B, only 17.3% of CCR2-deficient mice succumbed to PR/8 infection as compared to 78.4% of infected wildtype mice ($p < 0.005$ on days 14 to 21 pi). Likewise, body weight loss was significantly less in CCR2$^{-/-}$ mice on days 8, 9, and 11 post infection (Fig. 13A).
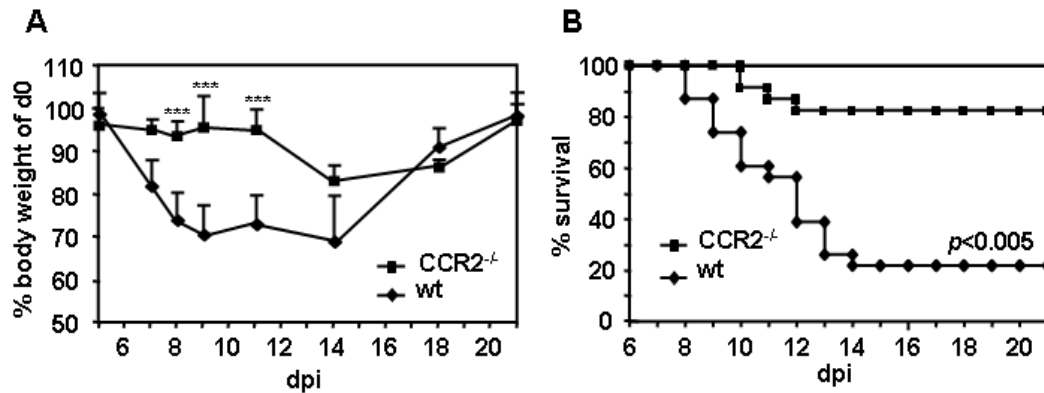
Fig. 13. CCR2 deficiency is associated with reduced body weight loss (A) and increased survival (B). Sex- and age-matched wt (♦, n=23) or CCR2$^{-/-}$ (■, n=23) mice were PR/8 infected at day 0 and body weight and survival were determined until day 21 pi.

To evaluate whether the observed differences in morbidity and mortality during PR/8 infection were associated with increased severity of lung injury in wildtype mice as compared to CCR2$^{-/-}$ mice, alveolar barrier function was assessed during a time course of 21 days post PR/8 infection in the two treatment groups. Indeed, alveolar leakage was significantly reduced in CCR2-deficient mice on day 7 post infection (1.25 ± 0.39 vs. 0.54 ± 0.37 AU, Fig. 14A). Correspondingly, treatment of infected wildtype mice with an anti-CCR2 mAb was associated with reduced alveolar leakage, as compared to isotype-treated mice on day 7 post infection (Fig. 14B), suggesting a key role of CCR2-dependently recruited mononuclear phagocytes in IV-induced lung barrier breakdown.
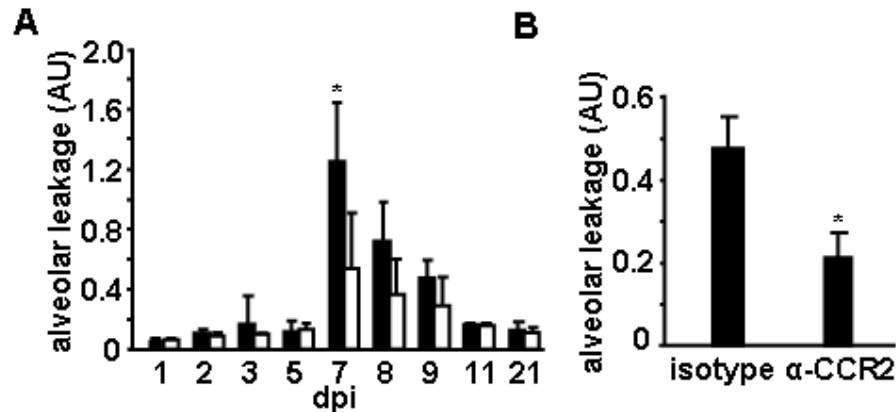
Fig. 14. Alveolar leakage in PR/8 infected wt (■) and CCR2$^{-/-}$ (□) mice (A) and in wildtype mice pretreated with IgG isotype or anti-CCR2 mAb (B). BALF and serum samples were taken from PR/8 infected mice at the indicated time point post infection 45 min after FITC-albumin injection and the lung permeability assay was performed. Values are given in means ± SD of n=3-5 animals per group; *p<0.05.

During IV pneumonia, alveolar epithelial injury may be caused by direct cytopathic effects of IV replicating primarily in epithelial cells. Therefore, we evaluated whether the observed differences in lung barrier damage between wildtype and CCR2-/- mice were linked to different viral replication efficiencies in the lung tissue of the two mouse strains. Analyses of viral replication in lung homogenates from PR/8 infected wildtype compared to CCR2$^{-/-}$ mice revealed no significant differences in peak viral titers at days 2, 3 and 5 post infection and even slightly elevated virus titers in CCR2$^{-/-}$ mice during later stages of infection (1.05 ± 1.33 x 10^3 versus 6.20 ± 3.90 x 10^3 FFU/lung on day 11 pi, Fig. 15).

These results indicate that enhanced alveolar injury in wildtype mice during PR/8 pneumonia is not due to higher viral replication rates than in CCR2$^{-/-}$ mice and rather suggest that mononuclear phagocytes recruited to inflamed tissues in a CCR2-dependent manner may directly cause alveolar damage during IV pneumonia.
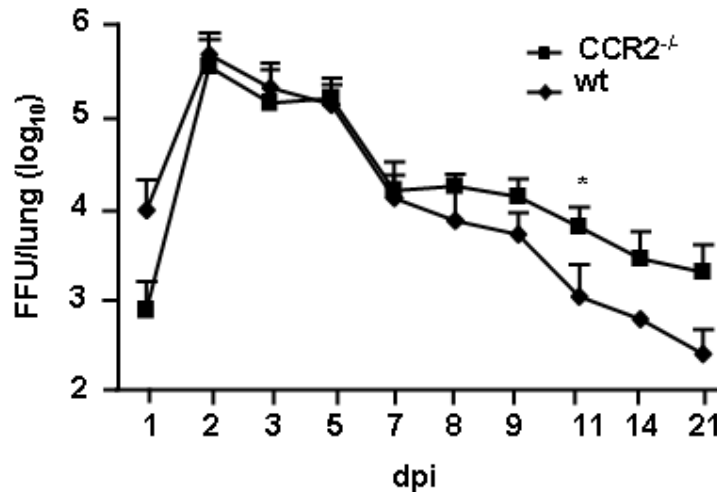
Fig. 15. **Lung virus titers of wt (♦) and CCR2$^{-/-}$ (■) mice in the time course of PR/8 infection.** PR/8 infected mice were sacrificed at the indicated time points post infection and virus titers were determined from lung homogenate supernatants. Values are given as foci forming units (FFU) per lung and are means ± SD from n=3-5 mice per group; * $p < 0.05$.

3.5 CCR2 expression on circulating leukocytes but not on lung resident cells is associated with alveolar barrier dysfunction during PR/8 infection

To distinguish whether CCR2 expressed on resident lung cells, such as resident alveolar macrophages or alveolar epithelial cells, or CCR2 present on circulating leukocytes accounted for the increased IV-induced alveolar leakage in wildtype vs. CCR2$^{-/-}$ mice, we made use of a bone marrow chimeric mouse model. We established three different transplantation groups: (i) wildtype mice which were transplanted 100% wildtype bone marrow cells, (ii) wildtype mice which were transplanted a mixture of wildtype and CCR2$^{-/-}$ bone marrow cells (50% wildtype/50% CCR2$^{-/-}$), and (iii) wildtype mice which were transplanted 100% CCR2$^{-/-}$ bone marrow cells. Bone marrow transplantation efficiency was analysed in CD45.1 alloantigen-expressing mice which were transplanted wildtype bone marrow cells (expressing the CD45.2 alloantigen, n=2 during each transplantation experiment) by calculating the proportion of CD45.2 positive donor peripheral blood leukocytes and of CD45.1 positive recipient resident alveolar macrophages by flow cytometry. Bone marrow engraftment was 90.5 ± 2.7% after two weeks post transplantation, whereas 92.2 ± 5.5% of resident alveolar macrophages exhibited a recipient phenotype (Fig. 16).
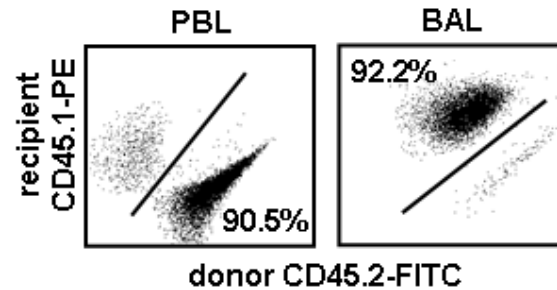
Fig.16. Analysis of transplantation efficiency in CD45.1 alloantigen expressing mice 14 days after transplantation of CD45.2 positive bone marrow. CD45.1 mice were lethally eradiated and transplanted 1.2 x 10^7 CD45.2 bone marrow cells by intravenous injection. Bone marrow engraftment of recipient CD45.1 mice was analysed 14d later in peripheral blood leukocytes by flow cytometry. Note, that resident alveolar macrophages were of recipient origin 14d post transplantation. Left panel: peripheral blood leukocytes (PBL), right panel: resident alveolar macrophages gained by BAL.

Exudate macrophage accumulation on day 8 post PR/8 infection in transplanted mice was dependent on the proportion of peripheral blood monocytes with intact CCR2 expression, with mice transplanted wildtype bone marrow recruiting 0.85 ± 0.27 x 10^6, mice transplanted mixed bone marrow recruiting 0.57 ± 0.29 x 10^6, and mice transplanted CCR2$^{-/-}$ bone marrow recruiting a total of 0.24 ± 0.09 x 10^6 exudate macrophages into the alveolar compartment (Fig. 17A). Fig. 17B shows a representative flow cytometry dot plot analysis of BAL leukocytes from the three treatment groups performed as described in chapter 3.3.
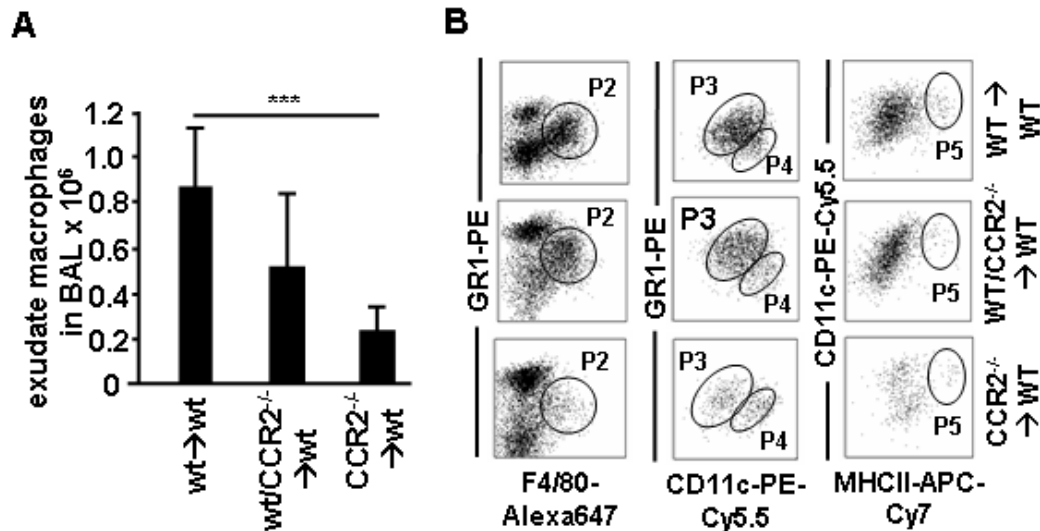
Fig. 17. Exudate macrophage recruitment is dependent on circulating monocyte-expressed CCR2. (A) Exudate macrophage numbers of the three different groups of PR/8 infected chimeric mice calculated from BALF leukocyte cell numbers and differential counts of Pappenheim-stained cytocentrifuge preparations. Values are given as means ± SD from n=4-8 mice per transplantation group; *** $p < 0.005$. **(B)** Flow cytometric analysis (representative experiment) of BALF cells from PR/8 infected chimeric mice. Note that P3 (exudate macrophages), P4 (resident alveolar macrophages), and P5 (alveolar dendritic cells) are subgates of P2 (mononuclear phagocytes).

Analysis of alveolar leakage at day 7 post infection revealed a significant reduction in mice transplanted mixed or 100% CCR2-/- bone marrow compared to mice transplanted 100% wildtype bone marrow. Of note, about 50% reduction of alveolar macrophage accumulation was sufficient to attenuate alveolar leakage to levels obtained in mice transplanted CCR2$^{-/-}$ bone marrow only (Fig. 18). These results clearly demonstrate that CCR2 expressed on circulating blood monocytes mediates their extravasation into the alveolar compartment of the lung, thereby contributing to alveolar barrier dysfunction during IV pneumonia.
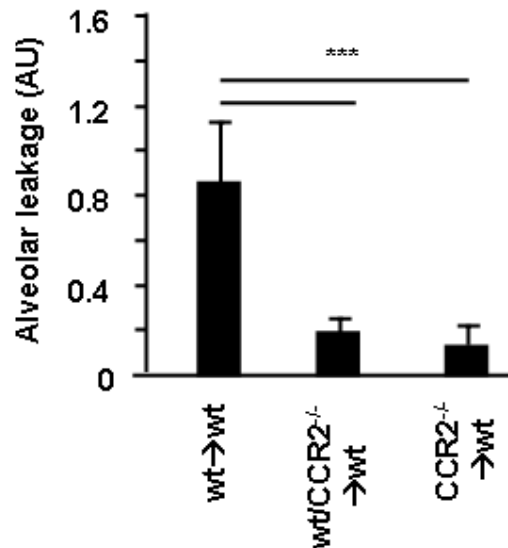
Fig. 18. Alveolar barrier dysfunction is associated with CCR2 expression on circulating monocytes during PR/8 infection. Alveolar leakage from PR/8 infected chimeric mice of the three different transplantation groups was determined by the lung permeability assay at d7 pi. All values are given as means ± SD from n=4-8 mice per transplantation group; *** *p* < 0.005.

3.6 CCR2-dependent alveolar exudate macrophage accumulation is associated with increased alveolar epithelial cell apoptosis

Given that the CCR2-dependent accumulation of exudate macrophages in IV pneumonia contributed to the loss of alveolar barrier integrity, we hypothesized that this recruited mononuclear cell population might promote barrier dysfunction by inducing alveolar epithelial apoptosis. Therefore, cryosections from lavaged lungs of mock- or PR/8-infected wildtype or CCR2-deficient mice were subjected to TUNEL assay. As shown in Figure 19A, the number of apoptotic alveolar cells was strikingly less in PR/8-infected CCR2$^{-/-}$ mice as compared to wildtype mice, and virtually undetectable in mock-infected wildtype or CCR2-deficient mice.

For apoptosis quantification of alveolar epithelial type I cells representing the major component of the alveolar surface, lung homogenates of the respective treatment groups were subjected to flow cytometry and CD45$^-$ cells were analysed for annexin V binding and expression of the alveolar epithelial cell type I marker T1α. Representative dot plots in Fig 19B (left panel) demonstrate a significantly larger proportion of type I alveolar epithelial cells to undergo apoptosis in lung homogenates of PR/8-infected wildtype mice (49.4 ± 14.3%) than in PR/8-infected CCR2-deficient mice (28.0 ± 8.7%). Notably,

CCR2$^{-/-}$ mice still exhibited a 28% alveolar epithelial apoptosis rate. Apoptosis of type I alveolar epithelial cells was undetectable in homogenates of mock-infected wildtype and CCR2$^{-/-}$ mice (Fig. 19C).
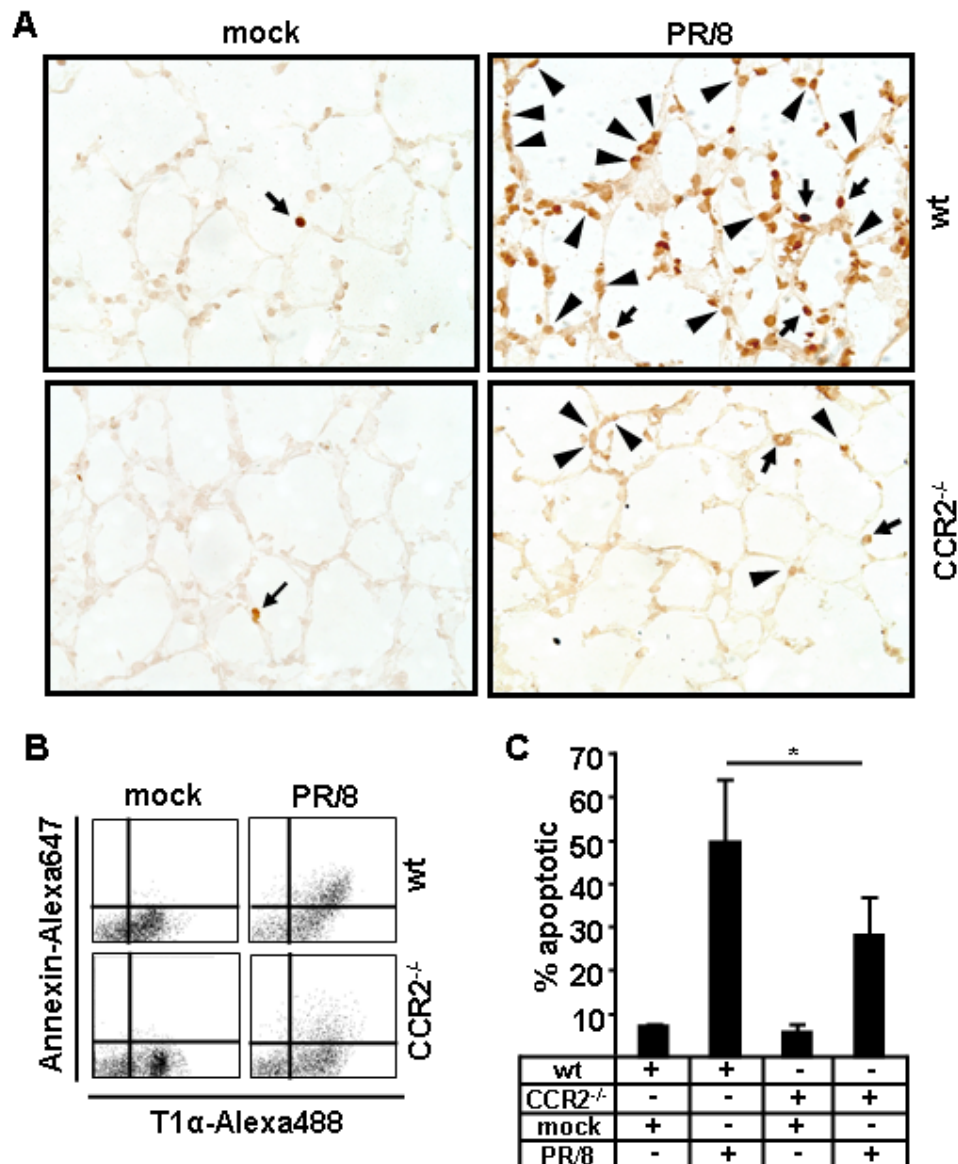

Fig. 19. (A) Alveolar epithelial cell apoptosis is reduced in PR/8 infected CCR2$^{-/-}$ mice as compared to wt mice, and virtually undetectable in mock infected mice. Note that nuclei of apoptotic cells appear in brown; arrow, apoptotic intraalveolar leukocyte; arrowhead, apoptotic alveolar epithelial cell; magnification x 400. **(B)** Flow cytometric quantification of apoptotic alveolar epithelial cells. Representative dot plots show expression of the alveolar epithelial cell type I marker T1α and annexin V staining of viable (propidium-iodide negative) CD45-negative cells. Note that apoptotic cells are mainly alveolar epithelial cells type I (left panel). **(C)** Quantification of flow cytometric data of n=3-6 mice per group; bar graphs represent the annexin V positive proportion of CD45-negative cells and are given as means ± SD; * $p < 0.05$.

3.7 Alveolar exudate macrophages upregulate mRNA levels of the proapoptotic TNF-related apoptosis-inducing ligand (TRAIL) as compared to peripheral blood monocytes

To analyse mRNA levels of potential proapoptotic factors in alveolar exudate macrophages and their blood precursors, peripheral blood monocytes from mock-infected or PR/8-infected wildtype mice as well as alveolar exudate macrophages from PR/8-infected wildtype mice were flow-sorted on day 8 post infection according to scatter and surface marker characteristics as shown in Fig. 20A and analysed for TNF-α, TRAIL, and FasL transcripts using quantitative RT-PCR. TNF-α mRNA transcripts were found to be significantly increased to the same level in both peripheral blood monocytes and alveolar exudate macrophages from PR/8-infected mice as compared to blood monocytes from mock-infected mice (Fig. 20B, left panel). However, TNF-α protein levels in BAL fluid did not significantly differ between PR/8-infected wildtype and CCR2-deficient mice (Fig. 20C), suggesting that exudate macrophages recruited to the alveolar space in wildtype but less in CCR2-/- mice were not the primary source of TNF-α. No significant upregulation of FasL mRNA could be detected in the analysed cell populations (Fig. 20B, middle panel). In contrast, TRAIL mRNA was selectively upregulated 4-fold in exudate macrophages as compared to their peripheral blood precursors from either mock- or PR/8-infected mice (Fig. 20B, right panel).
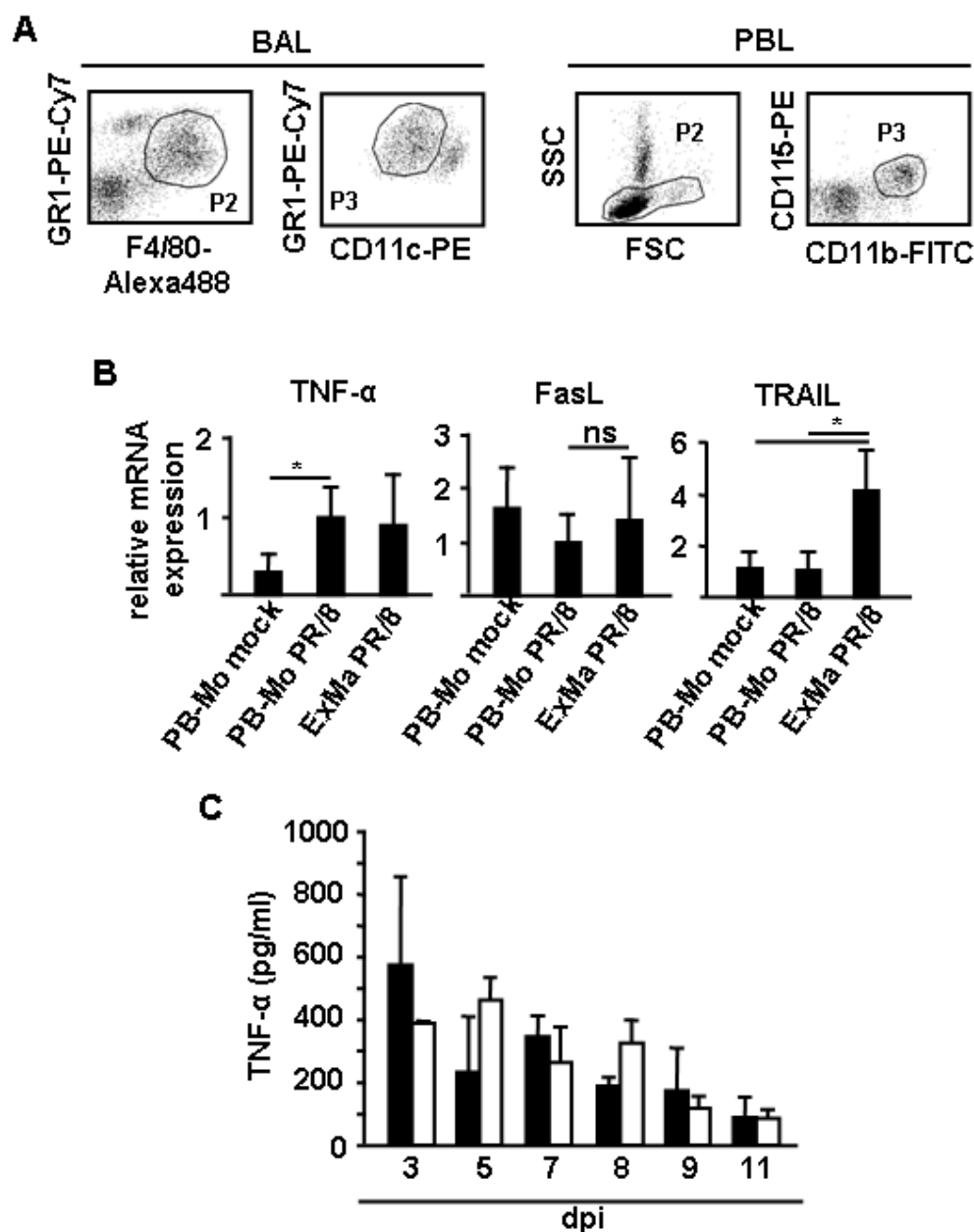
Fig. 20. Relative mRNA expression of the proapoptotic factors TNF-α, TRAIL and FasL in flow-sorted peripheral blood monocytes and alveolar exudate macrophages. (A) BALF exudate alveolar macrophages from PR/8 infected mice were high purity flow-sorted according to their surface expression of F4/80, GR1 and CD11c (F4/80$^+$GR1^{int}CD11c^{int}, P3, left panels). Peripheral blood monocytes from the same (PR/8 infected) animals or from mock-infected mice were flow-sorted according to their scatter characteristics (SSC^{low}) and their CD11b and CD115-expression (CD11b$^+$CD115$^+$, P3, right panels); SSC, side scatter; FSC, forward scatter. **(B)** Relative mRNA expression of the proapoptotic factors TNF-α, TRAIL and FasL of flow-sorted peripheral blood monocytes. Values are given as mean ± SD from n=3 independent experiments including pooled BALF or blood cells from n=8 mice each; * $p < 0.05$; ns, not significant. **(C)** Quantification of TNF-α protein levels in BALF of PR/8 infected wt (■) and CCR2$^{-/-}$ (□) mice.

3.8 TRAIL expression in the alveolar space is largely restricted to alveolar exudate macrophages during PR/8 infection

To evaluate TRAIL protein expression on the surface of alveolar mononuclear phagocytes, BALF cells from mock- or PR/8-infected wildtype or CCR2$^{-/-}$ mice were analysed by flow cytometry for F4/80 and TRAIL co-expression by day 8 post infection. TRAIL was exclusively found on F4/80$^+$ BALF cells from PR/8-infected wildtype but not CCR2-deficient mice, indicating that only CCR2-dependently recruited exudate macrophages, but not resident alveolar macrophages expressed TRAIL (Fig. 21A). The proportion of TRAIL$^+$ alveolar macrophages raised to ~14% in PR/8-infected wildtype mice on day 8 post infection and was always below 1.5% in CCR2-deficient mice in the time course of infection (Fig. 21B). As opposed to previous reports (57, 63), in our model, TRAIL was only expressed on a small proportion of alveolar NK cells and absent on alveolar CD4$^+$ and CD8$^+$ T cells as well as on alveolar neutrophils from both wildtype and CCR2$^{-/-}$ mice at the indicated time points (Fig. 22).
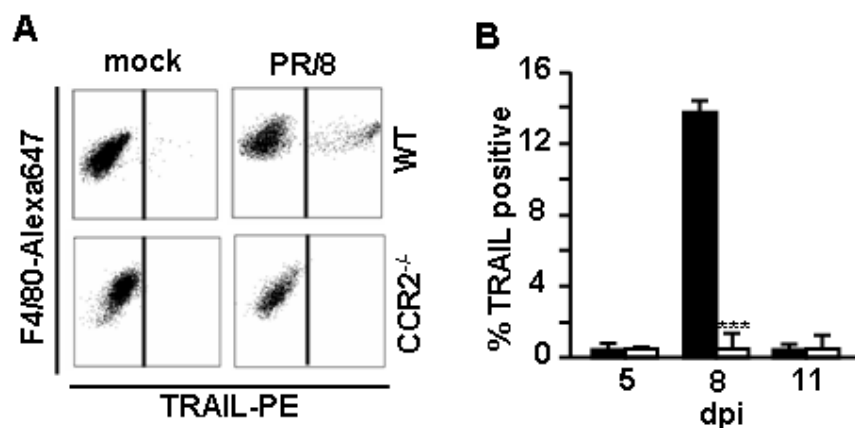
Fig. 21. TRAIL is expressed on the cell surface of alveolar exudate macrophages. (A) BAL leukocytes of mock or PR/8 infected wt or CCR2$^{-/-}$ mice were stained with GR1-FITC, F4/80-Alexa647 and TRAIL-PE or isotype-PE mAbs, respectively, for flow cytometric analysis of TRAIL expression on day 8 pi. GR1^{int}F4/80$^+$ cells were gated and analysed for their TRAIL surface expression. **(B)** Quantitative analysis of the proportion of TRAIL$^+$ from F4/80$^+$ BALF cells gained from PR/8-infected wt (■) or CCR2$^{-/-}$ (□) mice. Values are given as mean ± SD from n=3-4 mice per group; *** $p < 0.005$.
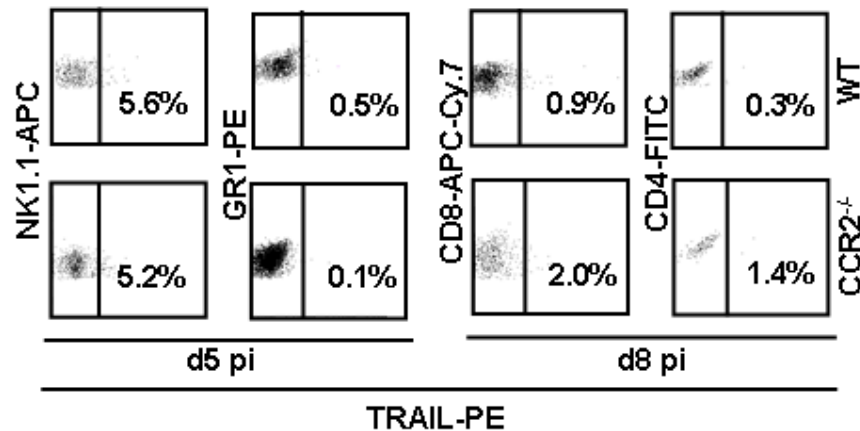
Fig. 22. Flow cytometric analysis of TRAIL expression on alveolar recruited cell populations. BAL leukocytes of PR/8-infected wt or CCR2$^{-/-}$ mice were subjected to flow cytometry and gated for NK-cells (SSC^{low}NK1.1^{+}), neutrophils (GR1^{high}F4/80^{-}), CD8 T cells (SSC^{low}CD8^{+}), and CD4 T cells (SSC^{low}CD4^{+}) and analysed for TRAIL expression.

3.9 Anti-TRAIL treatment attenuates alveolar epithelial apoptosis as well as lung leakage and enhances survival after PR/8 infection

To evaluate the contribution of exudate macrophage TRAIL to alveolar epithelial apoptosis, TUNEL assay was performed on cryosections of lavaged lungs from PR/8 infected wildtype mice treated with IgG isotype or anti-TRAIL mAb, respectively. As shown in Fig. 23A, alveolar cell apoptosis was pronounced in isotype-treated, but significantly decreased in anti-TRAIL-treated mice on day 7 post PR/8 infection. In addition, anti-TRAIL treatment significantly reduced annexin V binding of alveolar epithelial cells type I in PR/8 infected lung homogenates as compared to isotype-treated controls, as demonstrated in a representative flow cytometry dot plot (Fig. 23B) and in the quantitative analysis in Fig. 23C. Of note, alveolar epithelial cell apoptosis could not be completely abrogated by anti-TRAIL treatment, suggesting an additional role for TRAIL-independent epithelial apoptosis in PR/8 infected lungs possibly due to cytopathic effects by epithelial IV-replication itself (Fig. 23C).
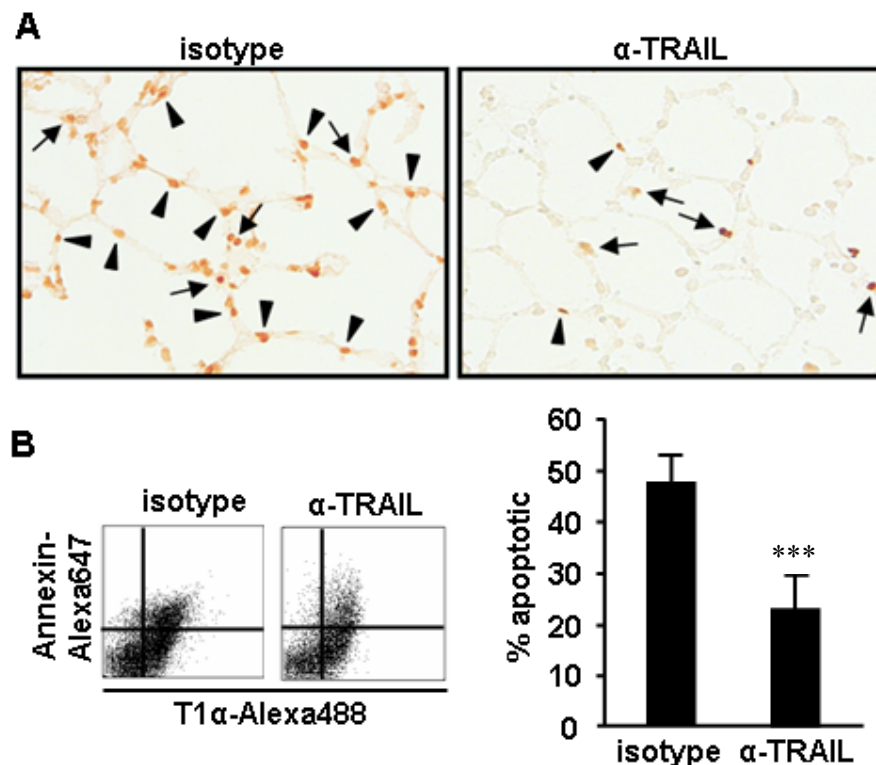
Fig. 23. Anti-TRAIL treatment attenuates alveolar epithelial cell apoptosis upon PR/8 infection. (A) PR/8-infected wt mice were treated with IgG isotype or anti-TRAIL mAb as described in *Materials and Methods* and TUNEL assay was performed from lung cryosections at day 7 pi (arrow, apoptotic intraalveolar leukocyte; arrowhead, apoptotic alveolar epithelial cell; magnification x 400). **(B)** Flow cytometric analysis of apoptotic type I alveolar epithelial cells from PR/8-infected isotype- or anti-TRAIL-treated mice was performed by annexin V binding. **(C)** Quantification of flow cytometric data was performed from n=3-6 mice per group; bar graphs represent the annexin V positive proportion of CD45-negative cells and are given as means ± SD; *** $p < 0.005$

Interestingly, TRAIL receptor (DR5) mRNA transcripts were found to be present in cultured primary murine alveolar epithelial cells and were upregulated upon PR/8 infection in a dose-dependent manner *in vitro* (Fig. 24A). Flow cytometric analysis of lung homogenates from PR/8 infected or non-infected wildtype mice revealed that 21.5 ± 1.3% of alveolar type I cells (CD45$^-$T1α$^+$) were PR/8 infected at d5 pi, as shown by IV nucleoprotein (NP) expression in a representative FACS dot plot in Fig. 24B. NP-positive alveolar type I epithelial cells showed an upregulated DR5 protein expression as compared to NP-negative type I cells (Fig. 24C).
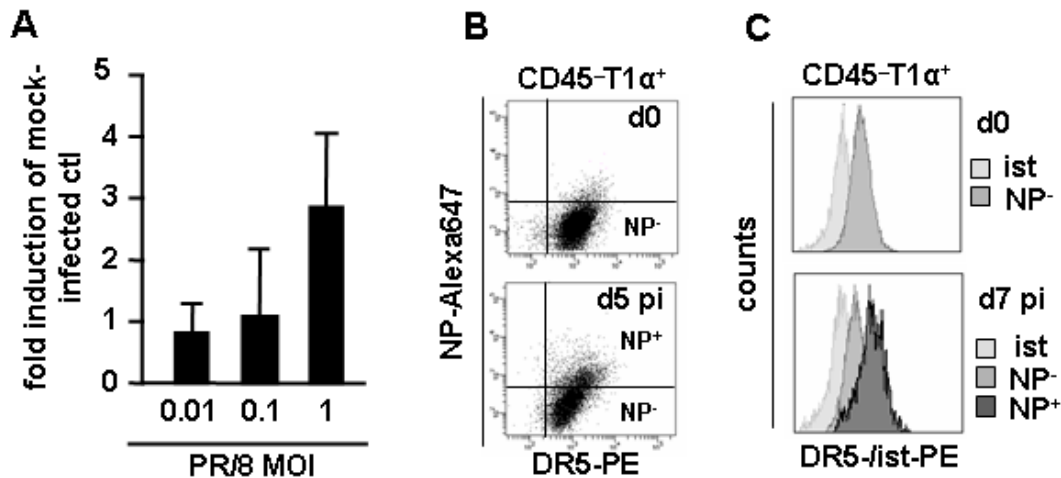
Fig. 24. TRAIL receptor (DR5) is expressed on isolated alveolar epithelial cells and upregulated upon PR/8 infection *in vitro* and *in vivo* . (A) Cultured primary AEC were either mock- or PR/8-infected with the indicated MOI for 8 h, and quantitative RT-PCR was performed. Bar graphs depict DR5 mRNA expression as fold induction of mock-infected alveolar epithelial cells. Values are given as means ± SD of n=3 independent experiments. **(B)** Lung homogenates from PR/8 infected (d5 pi) or non-infected (d0) wildtype mice were subjected to flow cytometry and CD45⁻T1α⁺ alveolar type I cells were gated and analysed for influenza nucleoprotein (NP) and DR5 expression. **(C)** Representative FACS histograms of DR5 expression on the surface of CD45⁻T1α⁺ alveolar type I cells in non-infected wildtype mice (d0) and in PR/8-infected wildtype mice at d7 pi (light grey, isotype control; medium grey, NP-negative type I cells; dark grey, NP-positive type I cells); ist, isotype.

Analysis of alveolar barrier function in anti-TRAIL treated, PR/8-infected wildtype mice revealed a significant decrease in alveolar leakage in comparison to isotype-treated control mice on day 7 post infection (Fig. 25A). Reduction of alveolar leakage in anti-TRAIL treated mice was associated with significantly increased survival of IV infection as compared to isotype-treated controls (Fig. 25B). These data clearly demonstrate a crucial role of TRAIL expressed by alveolar exudate macrophages in the development of alveolar barrier dysfunction as a major determinant of mortality during influenza virus pneumonia in mice.
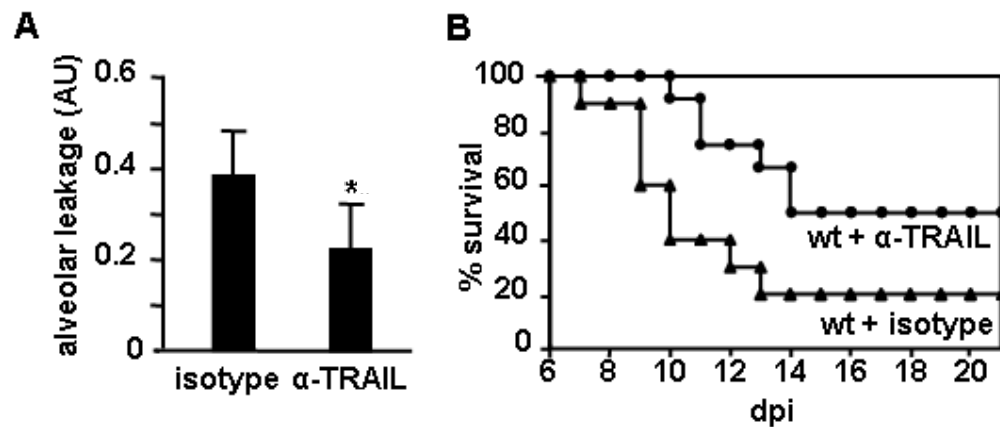
Fig. 25. Anti-TRAIL treatment attenuates alveolar leakage and enhances survival upon PR/8 infection. (A) PR/8-infected wt mice were treated with IgG isotype or anti-TRAIL mAb and sacrificed to perform the lung permeability assay on day 7 pi. Values are given as means ± SD from n=5 mice per group; * p = 0.05. **(B)** Survival of PR/8-infected wt mice treated with igG isotype or anti-TRAIL mAb was analysed until day 21 pi (p < 0.05).

4. Discussion

Mononuclear phagocytes of the lung, in particular newly recruited "exudate" macrophages, have been attributed a crucial role in host defense towards IV infection. Moreover, macrophages were considered to contribute to an imbalanced, detrimental immune response during IV pneumonia presumably resulting in alveolar epithelial damage and acute lung injury. In the present thesis, alveolar recruitment pathways of peripheral blood monocytes/macrophages upon influenza virus infection were analysed *in vitro* and *in vivo*, demonstrating a crucial role of the CCL2/CCR2 axis. Moreover, the hypothesis that exudate macrophages, recruited to the lung in a CCL2/CCR2-dependent manner, might contribute to lung barrier dysfunction during lethal influenza virus infection was tested. In fact, alveolar barrier function, severely disturbed in IV-infected wildtype mice, was found to be significantly less affected in CCR2-deficient mice exhibiting defective exudate macrophage recruitment. Consequently, CCR2-deficiency was associated with drastically decreased mortality during experimental IV pneumonia. Moreover, the pronounced lung leakage observed in wildtype mice correlated with an increased alveolar epithelial cell apoptosis rate found to be induced by the TNF-related apoptosis-inducing ligand (TRAIL) that is predominantly expressed in exudate lung macrophages. Finally, treatment of IV infected wildtype mice with an anti-TRAIL mAb not only attenuated alveolar leakage but significantly reduced mortality from IV pneumonia. Taken together, these results demonstrate that macrophage recruitment to IV-infected lungs in mice exerts detrimental effects on lung parenchymal cells of the highly sensitive gas exchange compartment, severely affecting alveolar barrier function via TRAIL-induced epithelial apoptosis (Fig. 26).

4.1 CCR2/CCL2 dependency of monocyte/macrophage lung recruitment *in vitro* and *in vivo*

The presented data demonstrate that influenza A virus infection of primary alveolar epithelial cells elicits a basal-to-apical monocyte transepithelial migration across infected epithelium *in vitro*. Although virus-infected alveolar epithelial cells displayed a pronounced release of both chemoattractants CCL2

and CCL5, monocyte transmigration across PR/8 infected epithelium was only dependent on monocyte CCR2 but not CCR5 receptor expression. Previous reports demonstrated an impaired monocyte recruitment into the lungs of CCR2 knockout but not CCL5 or CCR5 knockout mice upon influenza A virus infection *in vivo*, without addressing the contribution of distinct alveolar cell types to the mononuclear phagocyte trafficking in response to influenza A virus infection (14, 64, 65). The current data add to the aforementioned studies and provide evidence for an active role of virus-infected alveolar epithelial cells to elicit a basal-to-apical monocyte transepithelial migration in a CCL2 but not CCL5 dependent fashion, as demonstrated by the use of CCL2-neutralizing antibodies. Interestingly, the CCL2/CCR2 axis was found to be crucial for monocyte transmigration, as opposed to the role of CCR5. Thus, these findings demonstrate a major role of the CCL2/CCR2 axis in monocyte-epithelial interactions leading to monocyte recruitment across the influenza virus infected alveolar epithelial barrier. The fact that transmigration of CCR5-deficient monocytes across virus-infected epithelium was not affected when compared to wildtype monocytes strongly argues against a major contribution of CCL5 to monocyte transepithelial migration in our system, which is additionally supported by the findings that CCL2 release from influenza-infected epithelial cells exceeded the CCL5 release by a factor of 3, and by the observation that monocyte recruitment across mock-infected epithelium was much weaker in response to recombinant CCL5 as compared to CCL2.

Consistent with the presented *in vitro* data, exudate macrophage accumulation upon PR/8 infection *in vivo* was strictly dependent on monocyte-expressed CCR2. Although it has been reported that CCR2 might also bind CCL8, CCL16 and CCL26 (66-68), alveolar macrophage recruitment was most likely initiated via an interaction with its primary ligand CCL2, being released into the alveolar compartment to large amounts. Surprisingly, CCL2 secretion revealed to be > 10-fold higher in CCR2$^{-/-}$ mice than in wildtype mice, an effect which has been described previously, presumably resulting from reduced CCL2 consumption by invading macrophages (62).

The CCL2/CCR2 axis is known to play a crucial role in host defense against pathogens by mediating the recruitment of GR1^{+} peripheral blood monocytes to sites of infection, thereby expanding the resident mononuclear

phagocyte pool. CCR2$^{-/-}$ and CCL2$^{-/-}$ mice were found to be extremely susceptible to acute toxoplasmosis and were unable to survive typically nonlethal doses of a nonvirulent strain of *T. gondii* (38). In a model of hepatic CMV infection, CCL2- and CCR2-deficient mice in comparison to wildtype mice exhibited increased viral titers, widespread virus-induced liver pathology and succumbed to infection (69). Moreover, CCL2 overexpressing mice displayed an improved pneumococcal clearance and survival compared to wildtype mice associated with substantially increased lung mononuclear phagocyte subset accumulations upon pneumococcal challenge (33). In striking contrast, in the presented model, CCR2-deficiency was found to be associated with only a slight (yet significant) delay in PR/8 clearance confirming observations reported previously by Dawson et al. (14) who suggest delayed adaptive immune responses being the underlying mechanism. However, we were not able to detect significant differences in the alveolar accumulation of CD4$^+$ or CD8$^+$ T lymphocytes, despite the observed delay in dendritic cell recruitment, known as the major antigen-presenting cell population. These results are supported by the findings of Osterholzer and colleagues, demonstrating that immature DC recruitment to the lungs of mice in response to particulate antigen was only partially dependent on CCR2 (70). Of note, in the present thesis, persistent IV replication in CCR2$^{-/-}$ mice seemingly had no effect on alveolar epithelial integrity, emphazising the predominant role of host as opposed to pathogen factors in IV-induced pathology.

4.2 Contribution of CCR2-dependently recruited exudate macrophages to IV-induced acute lung injury

Influenza virus pneumonia is characterized by rapid development of acute lung injury with poor outcome. One of the hallmarks of acute lung injury is an incremental alveolar barrier dysfunction followed by accumulation of protein-rich edema fluid in the alveolar compartment (9, 71, 72), and acute respiratory distress syndrome (ARDS). ARDS is a clinical syndrome characterized by damage to the alveolo–capillary interface, usually secondary to an intense inflammatory response of the host lung to bacterial or viral infections. Several studies have demonstrated that respiratory infections lead to impairment of the alveolar epi- and endothelium, resulting in increased thickness of alveolo–

capillary membranes and decreased number of ventilated alveoli with reduced peripheral oxygenation (73, 74). Both viral pathogenicity factors and imbalanced host immune responses have been attributed a role in IV-induced ARDS (75, 76). It is believed that ARDS is a clinical syndrome secondary to an intense, usually neutrophil-predominant host inflammatory response (49). After stimulation by proinflammatory cytokines, activated neutrophils release free radicals, inflammatory mediators, and proteases, which lead to lung damage (73). However, in the presented model, it is clearly demonstrated that alveolar recruited neutrophils did not account for the severe alveolar damage observed in PR/8 infected mice, as neutrophils were recruited to the lungs of CCR2-deficient mice to a large extent, and even slightly exceeded alveolar neutrophil accumulation in wildtype mice. Thus, we assumed that the reduced lung leakage and mortality observed in CCR2-deficient mice during IV-infection might be attributed to abrogated pulmonary macrophage accumulation. In fact, as demonstrated by the use of chimeric mice, loss of alveolar barrier function was solely dependent on CCR2 expression on circulating monocytes, indicating that mononuclear phagocyte traffic was critically involved and that CCR2-positive resident lung cell populations, such as alveolar epithelial cells and resident alveolar macrophages, did not contribute to increased lung permeability in the presented model. Interestingly, a reduction of lung macrophage recruitment by 50% resulted in an approximately 5-fold decrease in alveolar leakage, suggesting that partial inhibition of macrophage recruitment during IV pneumonia may strongly attenuate lung injury while presumably maintaining critical macrophage host defense functions.

4.3 Role of exudate macrophage TNF-related apoptosis-inducing ligand (TRAIL) in acute lung injury upon IV pneumonia

Alveolar epithelial apoptosis has been described as a common feature of acute lung injury caused by direct or indirect factors, such as pneumonia, aspiration, sepsis or trauma (50-52, 77). Apoptosis is a regulated form of cell death that is mediated by membrane death receptors (extrinsic pathway) and direct mitochondrial injury (intrinsic pathway). Apoptosis has been described to occur in the lungs of patients with acute lung injury by activation of the epithelial membrane Fas death receptor by soluble Fas ligand (sFasL), released from

invading leukocytes and accumulating in biologically active form at the onset of lung injury (78-80). However, in our model of IV-induced acute lung injury, FasL transcripts were not significantly regulated in the macrophage subsets analysed. In contrast, the proapoptotic molecule TRAIL not expressed in peripheral blood monocytes was found to be strongly upregulated in exudate macrophages recruited into the alveolar space in IV-infected wildtype mice, whereas TRAIL was undetectable in alveolar mononuclear phagocytes of IV-infected CCR2$^{-/-}$ mice. TRAIL induction in alveolar exudate macrophages may be due to the recruitment process into the lung itself or to inflammatory mediators present within the IV-infected alveolar compartment. Previous reports identified type I interferons as potent inducers of TRAIL in monocytes and dendritic cells (59, 81). Indeed, in the presented study, interferon-α was alveolarly released upon PR/8 infection in wildtype mice, yet peaking early by day 2 post infection (219 ± 78pg/ml). TRAIL, acting as a membrane-bound or soluble form, has been known to induce apoptosis in various tumour cells, but not in non-neoplastic cells (58, 59). Recently, TRAIL expressed on lymphocyte subpopulations, dendritic cells and monocyte-derived macrophages has been associated with anti-viral host responses during IV-infection (56, 57, 82), underlining the importance of death pathways in anti-viral immunity. In contrast, Wurzer et al. found TRAIL-induced programmed cell death pathways to be crucial for IV propagation (83). In mice, TRAIL exclusively acts via the membrane death receptor 5 (DR5) expressed on the target cell. Interestingly, DR5 was upregulated in primary murine alveolar epithelial cells *in vitro* and *in vivo* upon PR/8 infection in a dose-dependent manner, suggesting that a preceding epithelial IV-infection might facilitate TRAIL-induced apoptosis as a potential host mechanism to limit viral spread. However, DR5 mRNA expression was also detectable in uninfected epithelial cells, suggesting that exudate macrophage TRAIL may have the potential to attack non-infected epithelial cells when released in large amounts.

Altogether, the present data demonstrate a key role of exudate macrophage TRAIL in alveolar epithelial cell apoptosis promoting alveolar barrier dysfunction during IV lung infection. Notably, inhibition of TRAIL activity largely protected mice from lethal influenza virus pneumonia. Targeting the

TRAIL-DR5 pathway might therefore be a suitable tool to restore lung epithelial function in patients suffering from severe IV-pneumonia.
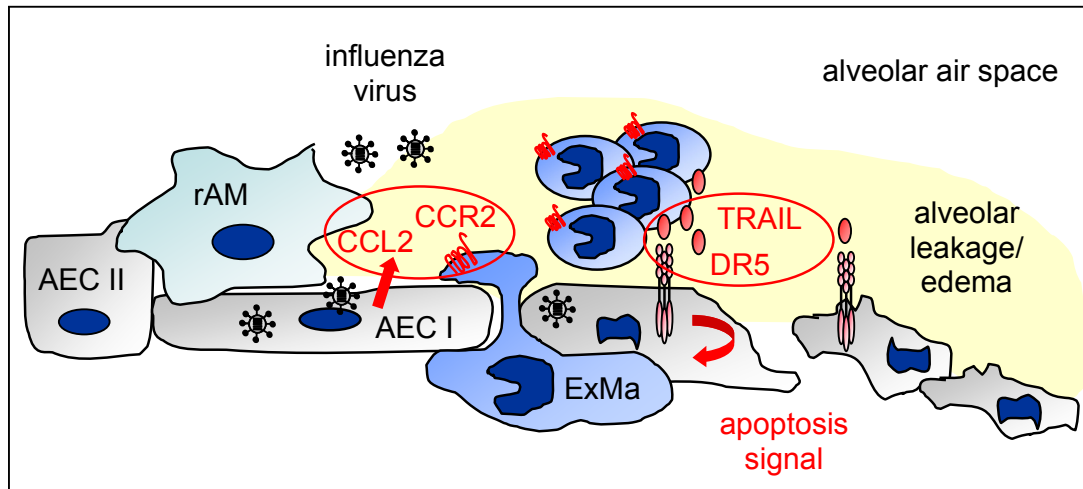
Fig. 26. Proposed model of macrophage-epithelial interactions during IV-induced acute lung injury: Peripheral blood monocytes are recruited in a CCL2/CCR2-dependent manner across PR/8-infected alveolar epithelial cells. Upon transepithelial migration into the alveolar air space, peripheral blood monocytes acquire an exudate macrophage phenotype and upregulate TRAIL, thereby inducing type I alveolar epithelial cell apoptosis. This process is supported by a PR/8-dependent upregulation of the TRAIL receptor DR5 on the alveolar epithelium. Alveolar epithelial cell apoptosis is followed by destruction of the thin alvoelo-capillary gas exchange barrier, accompanied by alveolar edema formation as a determinant of morbidity and mortality in IV-induced ALI.

5. Summary

Influenza A virus pneumonia is characterized by rapid progression to lung failure and high mortality. During early stages of infection significant amounts of leukocytes accumulate within the lung parenchyma including peripheral blood monocytes/macrophages, neutrophils and lymphocytes. Among these, macrophages have been attributed a crucial role in the host defense towards influenza virus (IV). In contrast, the precise transepithelial recruitment pathways of peripheral blood monocytes into the alveolar air space and the potential contribution of alveolarly accumulating ("exudate") macrophages to alveolar epithelial damage and lung barrier dysfunction during IV pneumonia has not yet been adequately addressed. Therefore, the present thesis investigated the chemokine-receptor involvement during IV-induced transepithelial monocyte migration *in vitro* and *in vivo*. Infection of primary murine alveolar epithelial cells with the mouse-adapted influenza A virus strain PR/8 markedly induced the release of the monocyte chemoattractants CCL2 and CCL5 followed by a strong monocyte transepithelial migration. This monocyte migratory response was strictly dependent on monocyte CCR2 but not CCR5 chemokine receptor expression. Moreover, using CCR2-deficient mice and function blocking anti-CCR2 antibodies in an IV pneumonia model, it was demonstrated that alveolar macrophage accumulation was solely dependent on monocyte-expressed CCR2 *in vivo*. In addition, the contribution of lung exudate macrophages to alveolar leakage formation during lethal IV pneumonia was delineated. Exudate macrophage accumulation in the lungs of PR/8 infected wildtype mice was associated with increased alveolar epithelial cell apoptosis, lung leakage and mortality. All these features of acute lung injury were strongly reduced in CCR2$^{-/-}$ mice and in wildtype mice treated with function blocking anti-CCR2 antibodies. Among several proapoptotic mediators analysed, TNF-related apoptosis-inducing ligand (TRAIL) gene expression was found to be markedly upregulated in alveolar exudate macrophages as compared to peripheral blood monocytes. Moreover, among the different alveolar recruited leukocyte subsets, TRAIL protein was predominantly expressed on macrophages. Finally, repetitive treatment of IV-infected mice with a monoclonal anti-TRAIL antibody resulted in

significant reduction of alveolar epithelial cell apoptosis, attenuated alveolar leakage and significantly increased survival.

Collectively, these findings demonstrate a major role of the CCL2/CCR2 axis in monocyte transepithelial migration. Additionally, CCR2-dependently recruited exudate macrophages were shown to be key players in the induction of alveolar leakage and mortality in influenza virus pneumonia, with macrophage TRAIL expression-linked epithelial apoptosis being recognized as major underlying mechanism and potential treatment target.

5. Zusammenfassung

Die Influenza A Viruspneumonie verläuft häufig rasch progredient bis hin zum akuten Lungenversagen und ist gekennzeichnet durch eine hohe Mortalität. In den frühen Stadien der Infektion kommt es zu einer ausgeprägten Rekrutierung von Monozyten/Makrophagen, neutrophilen Granulozyten und Lymphozyten ins Lungenparenchym. Insbesondere den Makrophagen wird eine bedeutende Rolle in der Immunabwehr gegen das Influenzavirus (IV) zugeschrieben. Jedoch waren die molekularen Pfade der transepithelialen Rekrutierung peripherer Blutmonozyten in den Alveolarraum und die mögliche Rolle dieser alveolär akkumulierenden Makrophagen bei der Induktion des pulmonalen Epithelschadens mit Verlust der alveolären Barrierefunktion bei der Influenzapneumonie bis dato ungeklärt. In der vorgelegten Arbeit wurden die der IV-induzierten transepithelialen Monozytenrekrutierung zugrundeliegenden Chemokin-Rezeptor-Interaktionen *in vitro* und *in vivo* analysiert. Die Infektion primärer muriner Alveolarepithelzellen mit dem Maus-adaptierten Influenza A Virus PR/8 induzierte eine ausgeprägte Freisetzung der Monozyten-rekrutierenden Chemokine CCL2 und CCL5 und eine deutliche transepitheliale Migration peripherer Blutmonozyten. Diese war strikt abhängig von monozytär exprimiertem CCR2, nicht jedoch von CCR5. In einem IV-Pneumonie Modell konnte darüber hinaus anhand CCR2-defizienter Mäuse und mittels Applikation von anti-CCR2-Antikörpern gezeigt werden, dass die alveoläre Makrophagenrekrutierung auch *in vivo* primär durch monozytär exprimiertes CCR2 vermittelt ist. Zusätzlich wurde der Beitrag alveolär rekrutierter Makrophagen zum Verlust der alveolären Schrankenfunktion in der IV-Pneumonie untersucht. Die Akkumulation rekrutierter Makrophagen in der IV-infizierten Lunge von Wildtyp-Mäusen ging einher mit signifikant vermehrter Alveolarepithelzellapoptose, verstärkter alveolärer Leakage und höherer Mortalität im Vergleich zu CCR2-defizienten Mäusen oder anti-CCR2-vorbehandelten Tieren. Die Analyse der Genexpression verschiedener pro-apoptotischer Faktoren ergab eine signifikante Hochregulation des TNF-related apoptosis-inducing ligand (TRAIL) in alveolär rekrutierten Makrophagen im Vergleich zu peripheren Blutmonozyten IV-infizierter Tiere, wobei TRAIL ausschliesslich auf der Oberfläche alveolärer Makrophagen, nicht jedoch auf

anderen alveolären Leukozytensubpopulationen exprimiert war. Schliesslich führte die repetitive Applikation eines monoklonalen anti-TRAIL-Antikörpers zu einer deutlichen Reduktion der alveolarepithelialen Apoptose, der alveolären Schrankenstörung und zum signifikant verbesserten Überleben IV-infizierter Tiere.

In der vorgelegten Arbeit konnte die CCL2/CCR2-Achse als wichtigster Signalpfad bei der IV-induzierten transepithelialen Monozyten-/Makrophagenrekrutierung identifiziert werden. Darüber hinaus konnte gezeigt werden, dass CCR2-abhängig alveolär rekrutierte Makrophagen durch die Expression des pro-apoptotischen Faktors TRAIL eine Schlüsselrolle in der Induktion der alveolarepithelialen Apoptose und des Zusammenbruchs der alveolären Schranke übernehmen und dabei wesentlich zur Mortalität bei der Influenza Viruspneumonie beitragen.

6. References

1.   2002. Influenza vaccines. *Wkly Epidemiol Rec 77:230*.

2.   Taubenberger, J. K., and D. M. Morens. 2006. 1918 Influenza: the mother of all pandemics. *Emerg Infect Dis 12:15*.

3.   Ghedin, E., N. A. Sengamalay, M. Shumway, J. Zaborsky, T. Feldblyum, V. Subbu, D. J. Spiro, J. Sitz, H. Koo, P. Bolotov, D. Dernovoy, T. Tatusova, Y. Bao, K. St George, J. Taylor, D. J. Lipman, C. M. Fraser, J. K. Taubenberger, and S. L. Salzberg. 2005. Large-scale sequencing of human influenza reveals the dynamic nature of viral genome evolution. *Nature 437:1162*.

4.   Hay, A. J., V. Gregory, A. R. Douglas, and Y. P. Lin. 2001. The evolution of human influenza viruses. *Philos Trans R Soc Lond B Biol Sci 356:1861*.

5.   Cox, N. J., and K. Subbarao. 1999. Influenza. *Lancet 354:1277*.

6.   Bender, B. S., and P. A. Small, Jr. 1992. Influenza: pathogenesis and host defense. *Semin Respir Infect 7:38*.

7.   Tran, T. H., T. L. Nguyen, T. D. Nguyen, T. S. Luong, P. M. Pham, V. C. Nguyen, T. S. Pham, C. D. Vo, T. Q. Le, T. T. Ngo, B. K. Dao, P. P. Le, T. T. Nguyen, T. L. Hoang, V. T. Cao, T. G. Le, D. T. Nguyen, H. N. Le, K. T. Nguyen, H. S. Le, V. T. Le, D. Christiane, T. T. Tran, J. Menno de, C. Schultsz, P. Cheng, W. Lim, P. Horby, and J. Farrar. 2004. Avian influenza A (H5N1) in 10 patients in Vietnam. *N Engl J Med 350:1179*.

8.   Cheung, T. K., and L. L. Poon. 2007. Biology of influenza a virus. *Ann N Y Acad Sci 1102:1*.

9.   Arabi, Y., C. D. Gomersall, Q. A. Ahmed, B. R. Boynton, and Z. A. Memish. 2007. The critically ill avian influenza A (H5N1) patient. *Crit Care Med 35:1397*.

10.   Cheung, C. Y., L. L. Poon, A. S. Lau, W. Luk, Y. L. Lau, K. F. Shortridge, S. Gordon, Y. Guan, and J. S. Peiris. 2002. Induction of proinflammatory cytokines in human macrophages by influenza A (H5N1) viruses: a mechanism for the unusual severity of human disease? *Lancet 360:1831*.

11.   Lee, D. C., C. Y. Cheung, A. H. Law, C. K. Mok, M. Peiris, and A. S. Lau. 2005. p38 mitogen-activated protein kinase-dependent hyperinduction of tumor necrosis factor alpha expression in response to avian influenza virus H5N1. *J Virol 79:10147*.

12.   Fujisawa, H., S. Tsuru, M. Taniguchi, Y. Zinnaka, and K. Nomoto. 1987. Protective mechanisms against pulmonary infection with influenza virus. I. Relative contribution of polymorphonuclear leukocytes and of alveolar macrophages to protection during the early phase of intranasal infection. *J Gen Virol 68 (Pt 2):425*.

13.   Hofmann, P., H. Sprenger, A. Kaufmann, A. Bender, C. Hasse, M. Nain, and D. Gemsa. 1997. Susceptibility of mononuclear phagocytes to influenza A virus infection and possible role in the antiviral response. *J Leukoc Biol 61:408*.

14.   Dawson, T. C., M. A. Beck, W. A. Kuziel, F. Henderson, and N. Maeda. 2000. Contrasting effects of CCR5 and CCR2 deficiency in the pulmonary inflammatory response to influenza A virus. *Am J Pathol 156:1951*.

15.   Doherty, P. C. 1996. Immune responses to viruses. In *Clinical Immunology, Principles and Practice*, Vol. 1. R. R. Rich, T. A. Fleisher, B. D. Schwarz, W. T. Shearer, and W. Strober, eds. St. Louis, Mosby-Year Book, Inc., p. 535

16.   Julkunen, I., K. Melen, M. Nyqvist, J. Pirhonen, T. Sareneva, and S. Matikainen. 2000. Inflammatory responses in influenza A virus infection. *Vaccine 19 Suppl 1:S32*.

17.   Virelizier, J. L., A. C. Allison, and G. C. Schild. 1979. Immune responses to influenza virus in the mouse, and their role in control of the infection. *Br Med Bull 35:65*.

18.   Lehmann, C., H. Sprenger, M. Nain, M. Bacher, and D. Gemsa. 1996. Infection of macrophages by influenza A virus: characteristics of tumour necrosis factor-alpha (TNF alpha) gene expression. *Res Virol 147:123*.

19.   Julkunen, I., T. Sareneva, J. Pirhonen, T. Ronni, K. Melen, and S. Matikainen. 2001. Molecular pathogenesis of influenza A virus infection and virus-induced regulation of cytokine gene expression. *Cytokine Growth Factor Rev 12:171*.

20. Matsukura, S., F. Kokubu, H. Kubo, T. Tomita, H. Tokunaga, M. Kadokura, T. Yamamoto, Y. Kuroiwa, T. Ohno, H. Suzaki, and M. Adachi. 1998. Expression of RANTES by normal airway epithelial cells after influenza virus A infection. *Am J Respir Cell Mol Biol 18:255*.

21. Sprenger, H., R. G. Meyer, A. Kaufmann, D. Bussfeld, E. Rischkowsky, and D. Gemsa. 1996. Selective induction of monocyte and not neutrophil-attracting chemokines after influenza A virus infection. *J Exp Med 184:1191*.

22. Bussfeld, D., A. Kaufmann, R. G. Meyer, D. Gemsa, and H. Sprenger. 1998. Differential mononuclear leukocyte attracting chemokine production after stimulation with active and inactivated influenza A virus. *Cell Immunol 186:1*.

23. Van Reeth, K. 2000. Cytokines in the pathogenesis of influenza. In *Vet Microbiol*, Vol. 74, p. 109.

24. Friedland, J. S. 1996. Chemokines in viral disease. *Res Virol 147:131*.

25. Baggiolini, M., B. Dewald, and B. Moser. 1997. Human chemokines: an update. *Annu Rev Immunol 15:675*.

26. Kuziel, W. A., S. J. Morgan, T. C. Dawson, S. Griffin, O. Smithies, K. Ley, and N. Maeda. 1997. Severe reduction in leukocyte adhesion and monocyte extravasation in mice deficient in CC chemokine receptor 2. *Proc Natl Acad Sci U S A 94:12053*.

27. Rot, A., and U. H. von Andrian. 2004. Chemokines in innate and adaptive host defense: basic chemokinese grammar for immune cells. *Annu Rev Immunol 22:891*.

28. Braciak, T. A., K. Bacon, Z. Xing, D. J. Torry, F. L. Graham, T. J. Schall, C. D. Richards, K. Croitoru, and J. Gauldie. 1996. Overexpression of RANTES using a recombinant adenovirus vector induces the tissue-directed recruitment of monocytes to the lung. *J Immunol 157:5076*.

29. Mack, M., J. Cihak, C. Simonis, B. Luckow, A. E. Proudfoot, J. Plachy, H. Bruhl, M. Frink, H. J. Anders, V. Vielhauer, J. Pfirstinger, M. Stangassinger, and D. Schlondorff. 2001. Expression and characterization of the chemokine receptors CCR2 and CCR5 in mice. *J Immunol 166:4697*.

30. Christensen, P. J., M. Du, B. Moore, S. Morris, G. B. Toews, and R. Paine, 3rd. 2004. Expression and functional implications of CCR2 expression on murine alveolar epithelial cells. *Am J Physiol Lung Cell Mol Physiol 286:L68*.

31. Murdoch, C., and A. Finn. 2000. Chemokine receptors and their role in inflammation and infectious diseases. *Blood 95:3032*.

32. Landsman, L., C. Varol, and S. Jung. 2007. Distinct differentiation potential of blood monocyte subsets in the lung. *J Immunol 178:2000*.

33. Winter, C., K. Taut, M. Srivastava, F. Langer, M. Mack, D. E. Briles, J. C. Paton, R. Maus, T. Welte, M. D. Gunn, and U. A. Maus. 2007. Lung-specific overexpression of CC chemokine ligand (CCL) 2 enhances the host defense to Streptococcus pneumoniae infection in mice: role of the CCL2-CCR2 axis. *J Immunol 178:5828*.

34. Sunderkotter, C., T. Nikolic, M. J. Dillon, N. Van Rooijen, M. Stehling, D. A. Drevets, and P. J. Leenen. 2004. Subpopulations of mouse blood monocytes differ in maturation stage and inflammatory response. *J Immunol 172:4410*.

35. Geissmann, F., S. Jung, and D. R. Littman. 2003. Blood monocytes consist of two principal subsets with distinct migratory properties. *Immunity 19:71*.

36. Ginhoux, F., F. Tacke, V. Angeli, M. Bogunovic, M. Loubeau, X. M. Dai, E. R. Stanley, G. J. Randolph, and M. Merad. 2006. Langerhans cells arise from monocytes in vivo. *Nat Immunol 7:265*.

37. Qu, C., E. W. Edwards, F. Tacke, V. Angeli, J. Llodra, G. Sanchez-Schmitz, A. Garin, N. S. Haque, W. Peters, N. van Rooijen, C. Sanchez-Torres, J. Bromberg, I. F. Charo, S. Jung, S. A. Lira, and G. J. Randolph. 2004. Role of CCR8 and other chemokine pathways in the migration of monocyte-derived dendritic cells to lymph nodes. *J Exp Med 200:1231*.

38. Robben, P. M., M. LaRegina, W. A. Kuziel, and L. D. Sibley. 2005. Recruitment of Gr-1+ monocytes is essential for control of acute toxoplasmosis. *J Exp Med 201:1761*.

39. Breslow, J. L. 1996. Mouse models of atherosclerosis. *Science 272:685*.

40. von Wulffen, W., M. Steinmueller, S. Herold, L. M. Marsh, P. Bulau, W. Seeger, T. Welte, J. Lohmeyer, and U. A. Maus. 2007. Lung Dendritic

Cells Elicited by Flt3-Ligand Amplify the Inflammatory Response to Lipopolysaccharide. *Am J Respir Crit Care Med*.

41. Fogg, D. K., C. Sibon, C. Miled, S. Jung, P. Aucouturier, D. R. Littman, A. Cumano, and F. Geissmann. 2006. A clonogenic bone marrow progenitor specific for macrophages and dendritic cells. *Science 311:83*.

42. Herold, S., W. von Wulffen, M. Steinmueller, S. Pleschka, W. A. Kuziel, M. Mack, M. Srivastava, W. Seeger, U. A. Maus, and J. Lohmeyer. 2006. Alveolar epithelial cells direct monocyte transepithelial migration upon influenza virus infection: impact of chemokines and adhesion molecules. *J Immunol 177:1817*.

43. Maus, U., J. Huwe, L. Ermert, M. Ermert, W. Seeger, and J. Lohmeyer. 2002. Molecular pathways of monocyte emigration into the alveolar air space of intact mice. *Am J Respir Crit Care Med 165:95*.

44. Taut, K., C. Winter, D. E. Briles, J. C. Paton, J. W. Christman, R. Maus, R. Baumann, T. Welte, and U. A. Maus. 2007. Macrophage Turnover Kinetics in the Lungs of Mice Infected with Streptococcus pneumoniae. *Am J Respir Cell Mol Biol*.

45. Finnberg, N., J. J. Gruber, P. Fei, D. Rudolph, A. Bric, S. H. Kim, T. F. Burns, H. Ajuha, R. Page, G. S. Wu, Y. Chen, W. G. McKenna, E. Bernhard, S. Lowe, T. Mak, and W. S. El-Deiry. 2005. DR5 knockout mice are compromised in radiation-induced apoptosis. *Mol Cell Biol 25:2000*.

46. Kash, J. C., T. M. Tumpey, S. C. Proll, V. Carter, O. Perwitasari, M. J. Thomas, C. F. Basler, P. Palese, J. K. Taubenberger, A. Garcia-Sastre, D. E. Swayne, and M. G. Katze. 2006. Genomic analysis of increased host immune and cell death responses induced by 1918 influenza virus. *Nature 443:578*.

47. Chavakis, T., T. Keiper, R. Matz-Westphal, K. Hersemeyer, U. J. Sachs, P. P. Nawroth, K. T. Preissner, and S. Santoso. 2004. The junctional adhesion molecule-C promotes neutrophil transendothelial migration in vitro and in vivo. *J Biol Chem 279:55602*.

48. Bernard, G. R. 2005. Acute respiratory distress syndrome: a historical perspective. *Am J Respir Crit Care Med 172:798*.

49. Ware, L. B., and M. A. Matthay. 2000. The acute respiratory distress syndrome. *N Engl J Med 342:1334*.

50. Perl, M., C. S. Chung, U. Perl, J. Lomas-Neira, M. de Paepe, W. G. Cioffi, and A. Ayala. 2007. Fas-induced pulmonary apoptosis and inflammation during indirect acute lung injury. *Am J Respir Crit Care Med 176:591*.

51. Kitamura, Y., S. Hashimoto, N. Mizuta, A. Kobayashi, K. Kooguchi, I. Fujiwara, and H. Nakajima. 2001. Fas/FasL-dependent apoptosis of alveolar cells after lipopolysaccharide-induced lung injury in mice. *Am J Respir Crit Care Med 163:762*.

52. Guinee, D., Jr., E. Brambilla, M. Fleming, T. Hayashi, M. Rahn, M. Koss, V. Ferrans, and W. Travis. 1997. The potential role of BAX and BCL-2 expression in diffuse alveolar damage. *Am J Pathol 151:999*.

53. Kerr, J. F., A. H. Wyllie, and A. R. Currie. 1972. Apoptosis: a basic biological phenomenon with wide-ranging implications in tissue kinetics. *Br J Cancer 26:239*.

54. Chen, G., and D. V. Goeddel. 2002. TNF-R1 signaling: a beautiful pathway. *Science 296:1634*.

55. Benedict, C. A., T. A. Banks, and C. F. Ware. 2003. Death and survival: viral regulation of TNF signaling pathways. *Curr Opin Immunol 15:59*.

56. Zhou, J., H. K. Law, C. Y. Cheung, I. H. Ng, J. S. Peiris, and Y. L. Lau. 2006. Functional tumor necrosis factor-related apoptosis-inducing ligand production by avian influenza virus-infected macrophages. *J Infect Dis 193:945*.

57. Ishikawa, E., M. Nakazawa, M. Yoshinari, and M. Minami. 2005. Role of tumor necrosis factor-related apoptosis-inducing ligand in immune response to influenza virus infection in mice. *J Virol 79:7658*.

58. Cretney, E., K. Takeda, H. Yagita, M. Glaccum, J. J. Peschon, and M. J. Smyth. 2002. Increased susceptibility to tumor initiation and metastasis in TNF-related apoptosis-inducing ligand-deficient mice. *J Immunol 168:1356*.

59. Griffith, T. S., S. R. Wiley, M. Z. Kubin, L. M. Sedger, C. R. Maliszewski, and N. A. Fanger. 1999. Monocyte-mediated tumoricidal activity via the tumor necrosis factor-related cytokine, TRAIL. *J Exp Med 189:1343*.

60. Falschlehner, C., C. H. Emmerich, B. Gerlach, and H. Walczak. 2007. TRAIL signalling: decisions between life and death. *Int J Biochem Cell Biol 39:1462*.

61. Corti, M., A. R. Brody, and J. H. Harrison. 1996. Isolation and primary culture of murine alveolar type II cells. *Am J Respir Cell Mol Biol 14:309*.

62. Maus, U. A., S. Wellmann, C. Hampl, W. A. Kuziel, M. Srivastava, M. Mack, M. B. Everhart, T. S. Blackwell, J. W. Christman, D. Schlondorff, R. M. Bohle, W. Seeger, and J. Lohmeyer. 2005. CCR2-positive monocytes recruited to inflamed lungs downregulate local CCL2 chemokine levels. *Am J Physiol Lung Cell Mol Physiol 288:L350*.

63. Wegner, C. D., R. H. Gundel, P. Reilly, N. Haynes, L. G. Letts, and R. Rothlein. 1990. Intercellular adhesion molecule-1 (ICAM-1) in the pathogenesis of asthma. *Science 247:456*.

64. Wareing, M. D., A. B. Lyon, B. Lu, C. Gerard, and S. R. Sarawar. 2004. Chemokine expression during the development and resolution of a pulmonary leukocyte response to influenza A virus infection in mice. *J Leukoc Biol 76:886*.

65. Wareing, M. D., A. Lyon, C. Inglis, F. Giannoni, I. Charo, and S. R. Sarawar. 2007. Chemokine regulation of the inflammatory response to a low-dose influenza infection in CCR2-/- mice. *J Leukoc Biol 81:793*.

66. Nomiyama, H., K. Hieshima, T. Nakayama, T. Sakaguchi, R. Fujisawa, S. Tanase, H. Nishiura, K. Matsuno, H. Takamori, Y. Tabira, T. Yamamoto, R. Miura, and O. Yoshie. 2001. Human CC chemokine liver-expressed chemokine/CCL16 is a functional ligand for CCR1, CCR2 and CCR5, and constitutively expressed by hepatocytes. *Int Immunol 13:1021*.

67. Ogilvie, P., S. Paoletti, I. Clark-Lewis, and M. Uguccioni. 2003. Eotaxin-3 is a natural antagonist for CCR2 and exerts a repulsive effect on human monocytes. *Blood 102:789*.

68. Vande Broek, I., K. Asosingh, K. Vanderkerken, N. Straetmans, B. Van Camp, and I. Van Riet. 2003. Chemokine receptor CCR2 is expressed by human multiple myeloma cells and mediates migration to bone marrow stromal cell-produced monocyte chemotactic proteins MCP-1, -2 and -3. *Br J Cancer 88:855*.

69.   Hokeness, K. L., W. A. Kuziel, C. A. Biron, and T. P. Salazar-Mather. 2005. Monocyte chemoattractant protein-1 and CCR2 interactions are required for IFN-alpha/beta-induced inflammatory responses and antiviral defense in liver. *J Immunol 174:1549*.

70.   Osterholzer, J. J., T. Ames, T. Polak, J. Sonstein, B. B. Moore, S. W. Chensue, G. B. Toews, and J. L. Curtis. 2005. CCR2 and CCR6, but not endothelial selectins, mediate the accumulation of immature dendritic cells within the lungs of mice in response to particulate antigen. *J Immunol 175:874*.

71.   Xu, T., J. Qiao, L. Zhao, G. Wang, G. He, K. Li, Y. Tian, M. Gao, J. Wang, H. Wang, and C. Dong. 2006. Acute respiratory distress syndrome induced by avian influenza A (H5N1) virus in mice. *Am J Respir Crit Care Med 174:1011*.

72.   Morty, R. E., O. Eickelberg, and W. Seeger. 2007. Alveolar fluid clearance in acute lung injury: what have we learned from animal models and clinical studies? *Intensive Care Med 33:1229*.

73.   Headley, A. S., E. Tolley, and G. U. Meduri. 1997. Infections and the inflammatory response in acute respiratory distress syndrome. *Chest 111:1306*.

74.   Londhe, V. A., J. A. Belperio, M. P. Keane, M. D. Burdick, Y. Y. Xue, and R. M. Strieter. 2005. CXCR2 is critical for dsRNA-induced lung injury: relevance to viral lung infection. *J Inflamm (Lond) 2:4*.

75.   Tumpey, T. M., C. F. Basler, P. V. Aguilar, H. Zeng, A. Solorzano, D. E. Swayne, N. J. Cox, J. M. Katz, J. K. Taubenberger, P. Palese, and A. Garcia-Sastre. 2005. Characterization of the reconstructed 1918 Spanish influenza pandemic virus. *Science 310:77*.

76.   Szretter, K. J., S. Gangappa, X. Lu, C. Smith, W. J. Shieh, S. R. Zaki, S. Sambhara, T. M. Tumpey, and J. M. Katz. 2007. Role of host cytokine responses in the pathogenesis of avian H5N1 influenza viruses in mice. *J Virol 81:2736*.

77.   Uiprasertkul, M., R. Kitphati, P. Puthavathana, R. Kriwong, A. Kongchanagul, K. Ungchusak, S. Angkasekwinai, K. Chokephaibulkit, K. Srisook, N. Vanprapar, and P. Auewarakul. 2007. Apoptosis and

pathogenesis of avian influenza A (H5N1) virus in humans. *Emerg Infect Dis 13:708*.

78. Martin, T. R., M. Nakamura, and G. Matute-Bello. 2003. The role of apoptosis in acute lung injury. *Crit Care Med 31:S184*.

79. Martin, T. R., N. Hagimoto, M. Nakamura, and G. Matute-Bello. 2005. Apoptosis and epithelial injury in the lungs. *Proc Am Thorac Soc 2:214*.

80. Albertine, K. H., M. F. Soulier, Z. Wang, A. Ishizaka, S. Hashimoto, G. A. Zimmerman, M. A. Matthay, and L. B. Ware. 2002. Fas and fas ligand are up-regulated in pulmonary edema fluid and lung tissue of patients with acute lung injury and the acute respiratory distress syndrome. *Am J Pathol 161:1783*.

81. Liu, S., Y. Yu, M. Zhang, W. Wang, and X. Cao. 2001. The involvement of TNF-alpha-related apoptosis-inducing ligand in the enhanced cytotoxicity of IFN-beta-stimulated human dendritic cells to tumor cells. *J Immunol 166:5407*.

82. Chaperot, L., A. Blum, O. Manches, G. Lui, J. Angel, J. P. Molens, and J. Plumas. 2006. Virus or TLR agonists induce TRAIL-mediated cytotoxic activity of plasmacytoid dendritic cells. *J Immunol 176:248*.

83. Wurzer, W. J., C. Ehrhardt, S. Pleschka, F. Berberich-Siebelt, T. Wolff, H. Walczak, O. Planz, and S. Ludwig. 2004. NF-kappaB-dependent induction of tumor necrosis factor-related apoptosis-inducing ligand (TRAIL) and Fas/FasL is crucial for efficient influenza virus propagation. *J Biol Chem 279:30931*.

7. Supplement

7.1 Materials and source of supply

Abbocath	Abbott
AEC staining kit	Sigma
Aequous mounting medium	Dako
Agarose, low-melting	Sigma-Aldrich
Ammoniumchloride solution	Merck
Antibiotics (Pen/Strep)	PAA
a-hamster-Alexa 488 IgG	Molecular Probes
a-human/mouse pro-SPC mAb	Chemicon
anti-influenza nucleoprotein mAb	Biodesign
a-mouse biotinylated CD8α mAb	BD Pharmingen
a-mouse biotinylated I-A/I-E mAb	BD Pharmingen
a-mouse CCL2 mAb	R&D systems
a-mouse CD4-FITC mAb	BD Pharmingen
a-mouse CD4 MACS mAb	Miltenyi Biotech
a-mouse CD8 MACS mAb	Miltenyi Biotech
a-mouse CD11b-FITC mAb	BD Pharmingen
a-mouse CD11c-PE mAb	BD Pharmingen
a-mouse CD11c-PE-Cy5.5 mAb	Caltag
a-mouse CD19 MACS mAb	Miltenyi Biotech
a-mouse CD45.2-FITC mAb	BD Pharmingen
a-mouse CD45.1-PE mAb	BD Pharmingen
a-mouse CD45.2- PercP-Cy5.5 mAb	BD Pharmingen
a-mouse CD115-PE mAb	Serotec
a-mouse DR5 mAb	R&D
a-mouse F4/80-Alexa647 mAb	Caltag
a-mouse F4/80-Alexa488 mAb	Caltag
a-mouse GR1-FITC mAb	BD Pharmingen
a-mouse GR1-PE mAb	BD Pharmingen
a-mouse GR1-PE-Cy7 mAb	BD Pharmingen
a-mouse NK1.1-APC mAb	BD Pharmingen
a-mouse T1α/Podoplanin/gp36	Abcam

a-mouse TRAIL mAb (LEAF)	Biolegend
a-mouse TRAIL-PE mAb	Biolegend
a-mouse widespread cytokeratin mAb	Dako
annexin V-Alexa647	Molecular Probes
a-IV nucleoprotein mAb	Biodesign
Biotinylated a-mouse CD16/32 mAb	BD Pharmingen
Biotinylated a-mouse CD45 mAb	BD Pharmingen
Bovine serum albumin (BSA)	Sigma
$CaCl_2$	Roth
Cell culture plates/transwells	BD Biosciences
Colorimetric sandwich ELISA kits	R&D systems
DDT (Dithiotreitol)	Invitrogen
DeadEnd® Colorimetric TUNEL system	Promega
dH_2O	Pharmacia & Upjohn
Dispase	Beckton Dickinson
DNAse	Serva
DNTPs	Roche
Dulbecco´s modified eagle medium (DMEM)	PAA
EDTA	Biochrom
EDTA tubes	Sarstedt
Fc-Block	BD Pharmingen
Fetal calf serum (FCS)	Gibco
FITC-Albumin	Sigma
Hank´s buffered saline solution (HBSS)	PAA
Hepes buffer	Gibco
HRP-conjugated anti-mouse IgG	Santa Cruz Biotechnology
IgG2b rat isotype control antibody (azide-free)	BD Pharmingen
Isoflurane	Abbott
isotype-PE (rat IgG2aκ)	Biolegend
Ketamin hydrochloride (Ketavet®)	Pharmacia & Upjohn
LEAF IgG2a rat isotype control antibody	Biolegend
Leibovitz L15 medium	Gibco
Lympholyte®	Biozol
MACS columns	Miltenyi Biotech

Methylcellulose	Fluka Biochemika
$MgCl_2$	Roth
MMLV-Reverse Transcriptase	Invitrogen
NaCl 0.9%	Pharmacia & Upjohn
NaCl powder	Roth
Pappenheim staining solutions (May-Grünwald/Giemsa)	Merck
PE-conjugated anti-rat IgG	Serotec
PeqGold Total RNA kit	PeqLab
PFA (paraformaldehyde)	Sigma
Phosphate-buffered saline (PBS)	PAA
Platinum SYBR® Green qPCR SuperMix	Invitrogen
Random Hexamers	Böhringer Mannheim
rat IgG isotype antibody	BD Pharmingen
Recombinant murine CCL2	Peprotech
Recombinant murine CCL5	R&D systems
RLT buffer/ß-mercaptoethanol	Quiagen
Rnase InhibitoR	Promega
RNeasy Micro Kit	Qiagen
RPMI 1640 medium	PAA
SA-APC-Cy7	BD Pharmingen
Saponin	Calbiochem
5x 1st strand buffer	Invitrogen
Streptavidin-linked MagneSphere® Paramagnetic Particles	Promega
SYBR® Green	Invitrogen
Syringes	Braun Melsungen
TissueTek OCT	Sakura
Transgenic/mutated mice ($CCR2^{-/-}$, $CCR5^{-/-}$, CD45.1)	The Jackson Laboratory
Triton X-100	Sigma
Trypan blue	Sigma
Trypsin	PAA
Tween 20	Sigma

Ultra low cluster cell culture plates	Costar
Wildtype mice (BALB/c; C57/BL6)	Charles River
Xylazin hydrochloride (Rompun®)	Bayer

7.2 Technical equipment and manufacturer

ABI 7900 Sequence Detection System	Applied Biosystems
Cell Culture Incubator	Hereus
Centrifuges	Heraeus
Cytocentrifuge	Shandon
Digital Imaging Software	Leica
FACSCanto	Becton Dickinson
FACSDiva Software Package	Becton Dickinson
FACSVantage	Becton Dickinson
Fluorescence Spectrometer FLx800	Bio-Tek Instruments
Leica DM 2000 Light Microscope	Leica
Microplate Reader	Molecular Devices
PE GeneAmp PCR System 2400	Perkin Elmer
96-well Plate Autowasher	Tecan

8. Acknowledgements

9. Curriculum Vitae

Name   Dr. Susanne Valerie Herold

Date of birth   November 10th, 1975

Place of birth   Offenburg, Germany

Education/Training:

1995   Abitur, Gymnasium Gengenbach

1995-2002   Study of Human Medicine, University of Giessen

Since 2002   Assistenzärztin, Department of Internal Medicine II, Pulmonary and Critical Care Medicine and Infectious Diseases, UKGM

June 2002   Dissertation (Dr. med, MD) "Transendo-/epitheliale Rekrutierung von Monozyten in die Lunge: Phänotypische und funktionelle Charakterisierung"

2003-2006   International Graduate Program "Molecular Biology and Medicine of the Lung" (MBML) as part of the Giessen Graduate School of the Life Sciences (GGL)

2004-2007   PhD Program of the Faculties of Human and Veterinary Medicine of the University of Giessen

Scientific Awards/Prizes:

2006   Young Investigator´s Award of the German Society of Internal Medicine (DGIM)

2007   Scholarship of the Excellence Cluster Cardio-Pulmonary System (ECCPS)

2008   Best Poster Presentation Award of the 6th ERS Lung Science Conference on Lung Injury, Repair and Remodelling

Current Projects:

2007   Project Leader, Clinical Research Group "Pneumonie-Molekulare Signaturen kompartimentalisierter und schrankenübergreifender alveolärer Infektion" (BMBF)

2007   Associate Project Leader „FluResearchNet: Molecular signatures determining pathogenicity and species transmission of influenza A viruses" (BMBF)

Publications:

1. Maus UA, **Herold S**, Schlingensiepen KH, Schlingensiepen R, Dormayr T, Rosseau S, Maus R, Seeger W, Lohmeyer J. Antisense oligomers for selective suppression of MCP-1 synthesis in human pulmonary endothelial cells. Antisense Nucleic Acid Drug Dev. 10:185-93, 2000.

2. Maus U**, Herold S**, Muth H, Maus R, Ermert L, Ermert M, Weissman N, Rosseau S, Seeger W, Grimminger F, Lohmeyer J. Monocytes recruited into the alveolar air space of mice show a monocytic phenotype but upregulate CD14. Am J Physiol Lung Cell Mol Physiol. 280:L58-68, 2001.

3. **Herold S**., Friese G., Discher T., Enke B., Ghofrani A., Olschewski H., Lohmeyer J., Seeger W.: Bosentan plus Sildenafil in der Therapie der HIV-assoziierten pulmonalen Hypertonie. Erschienen in Eur J Med Res, Vol. 8 (Suppl. I) 2003, S. 66, Abstract N° 155.

4. **Herold S**, von Wulffen W, Steinmueller M, Pleschka S, Kuziel WA, Srivastava M, Seeger W, Maus UA, Lohmeyer J. Alveolar epithelial cells direct monocyte transepithelial migration upon influenza virus infection: Impact of chemokines and adhesion molecules. J. Immunol. 177:1817-24, 2006

5. Von Wulffen W, Steinmueller M, **Herold S,** Lohmeyer J, Seeger W, Maus UA. Flt3L elicited lung dendritic cells are recruited via b2 integrin pathways and amplify the lung inflammatory response to lipopolysaccharide. Am. J. Respir. Crit. Care Med. 176(9):892-901, 2007.

6. Ahlbrecht K, Schmitz J, Seay U, Mitnacht-Kraus R, Gaumann A, Haberberger RV, **Herold S**, Breier G, Seeger W, Voswinckel R. Spatiotemporal expression of flk-1 in pulmonary epithelial cells during lung development. Am. J. Respir. Cell Mol. Biol. 2008 Mar 6. Epub ahead of print.

7. **Herold S**, Steinmueller M, von Wulffen W, Cakarova L, Pinto R, Pleschka S, Mack M, Kuziel WA, Seeger W, Lohmeyer J. Lung epithelial apoptosis

in influenza virus pneumonia: The role of macrophage TNF-related apoptosis-inducing ligand. J. Exp. Med., in revision.

10. Declaration

I declare that I have completed this dissertation single-handedly without the unauthorized help of a second party and only with the assistance acknowledged therein. I have appropriately acknowledged and referenced all text passages that are derived literally from or are based on the content of published or unpublished work of others, and all information that relates to verbal communications. I have abided by the principles of good scientific conduct laid down in the charter of the Justus Liebig University of Giessen in carrying out the investigations described in the dissertation.

_____   _____

Place and Date   Dr. Susanne Herold